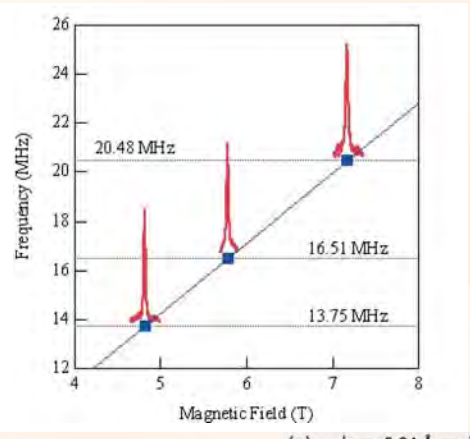

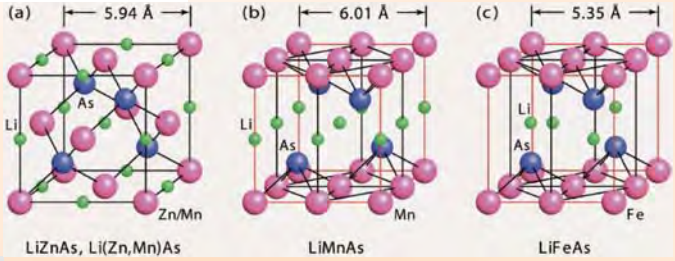

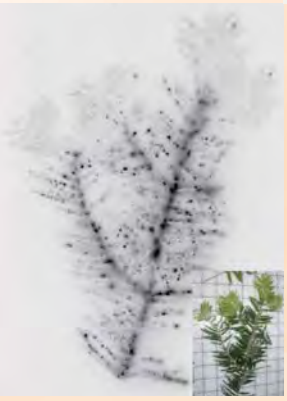

Annual Report of ASRC 2011

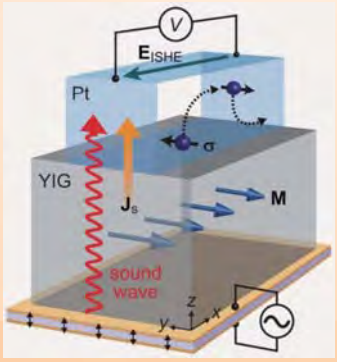

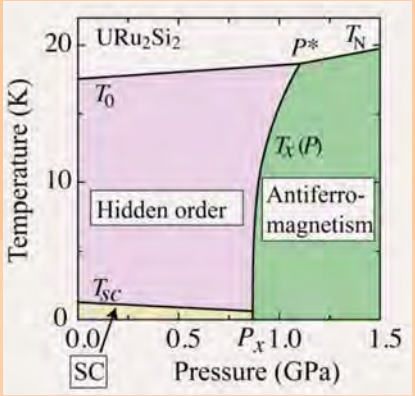

Advanced Science Research Center
Japan Atomic Energy Agency

Preface

Sadamichi Maekawa
Director General, Advanced Science Research Center

This issue contains the Annual Report of the Advanced Science Research Center (ASRC) activities for the fiscal year 2011. This is the second year of the five-year project cycle. Included in the issue are seven research highlights and a summary of the research of our eleven research groups.

The Great East Japan Earthquake of March 11, 2011 has had a significant impact on the various activities of the ASRC. Fortunately, the center suffered no fatalities. Due to the diligent efforts of its members and, especially, because of the support and encouragement given by the colleagues and institutes in the domestic and international communities in the relevant research fields, by October 2011, most of the experimental facilities of the ASRC had been restored and by January 2012, those of J-PARC.

For the restoration of the nuclear accident at the Fukushima Daiichi Nuclear Power Plant, the JAEA has been significantly contributing by making full use of equipments, research institutions and man power of JAEA. The ASRC members have been involving in technical contributions and serving in the general support activities such as measurement of contamination in the field and telephone counseling.

In addition to the community service, the ASRC members have made solid progress in their research. On behalf of the ASRC, I would like to express sincere appreciation to the generous support and collaborations which the members had enjoyed in this fiscal year during the time the experimental facilities of JAEA were not available due to the Earthquake. Needless to say, a great part of the progress presented in this Report reflects this support and collaborations.

Pictures on Cover Page:

❶ Sketch of the experimental procedure: For several constant frequency values f (purple solid horizontal lines), ^{239}Pu field-swept NMR spectra were obtained (red solid lines) mapping the pairs of f, B_{res} values that satisfy the resonance condition $2\pi f = \gamma_n (PuO_2) \cdot B_{res}$ (solid squares).

❷ Crystal structures of (a) semiconductor LiZnAs, ferromagnetic metal Li(Zn, Mn)As, (b) antiferromagnet LiMnAs and (c) non-magnetic superconductor LiFeAs.

❸ Autoradiograph image and optical photograph of *Torreya nucifera* sampled at Iitate, Fukushima, about 30 km from FDNPP. Black points in the autoradiograph image show the radioactive Cs is accumulated.

❹ Schematic illustration of the device structure to realize the new way of spin current generation by sound waves.

❺ Temperature pressure phase diagram in URu_2Si_2. "SC" indicates the superconducting phase. Application of pressure induces first order phase transition from hidden order to antiferromagnetic state.

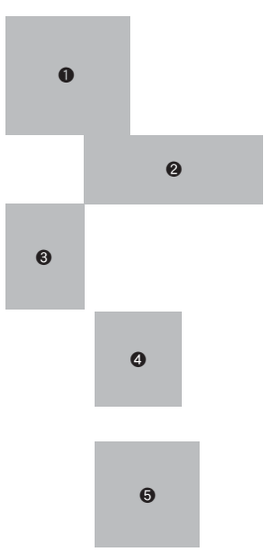

Contents

Organization of ASRC

JAEA

●Evaluation Committee of Research Activities for Advanced Science Research

Evaluation of R&D Themes

Advanced Science Research Center

Director General: Sadamichi Maekawa

Deputy Director General: Yuichiro Nagame

●Advisors:
Naoto Nagaosa (The University of Tokyo)
Samuel Bader (ANL, USA)

●Reimei Research Evaluation Committee

Research Coordination and Promotion Office
General Manager : Tomotsugu Sawai

※R.G.= Research Group

Advanced Materials Research

R.G. for Condensed Matter Theory
Group Leader : Michiyasu Mori

R.G. for Molecular Spintronics
Group Leader : Seiji Sakai

R.G. for Mechanical Control of Materials and Spin Systems
Group Leader : Eiji Saitoh

Frontier Research on Heavy Element System

R.G. for Reactions Involving Heavy Nuclei
Group Leader : Satoshi Chiba

R.G. for Superheavy Elements
Group Leader : Matthias Schädel

R.G. for Actinide Materials Sience
Group Leader : Zachary Fisk

R.G. for Condensed Matter Physics of Heavy Element Systems
Group Leader : Shinsaku Kambe

Research on Radiation Field Effects

R.G. for Hadron Physics
Group Leader : Ken-ichi Imai

R.G. for Bioactinide
Group Leader : Toshihiko Ohnuki

R.G. for Radiation and Biomolecular Science
Group Leader : Akinari Yokoya

R.G. for Spin-Polarized Positron Beam
Group Leader : Atsuo Kawasuso

Discovery of simple and versatile methods for spin current generation

H. Adachi[1,2)], J. Ieda[1,2)], S. Takahashi[3)], K. Uchida[3)], K. Ando[3)], E. Saitoh[2,3,4)], and S. Maekawa[1,2)]
1) R. G. for Condensed Matter Theory, ASRC, JAEA 2) CREST, JST. 3) Tohoku University
4) R. G. for Mechanical Control of Materials and Spin Systems, ASRC, JAEA

Electronics is indispensable in our daily life in the information society. As the next-generation technology, "spintronics" has attracted global interest. The "spin current" is the main ingredient of spintronics, and we have devised simple and versatile methods of generating spin current.

As the name implied, electronics is the art of controlling electrons in solids. The electron has two aspects: "charge" and "spin". The charge is the origin of electricity, and its flow leads to an electric (charge) current. On the other hand, the spin gives rise to magnetism and its flow is called a spin current. To date, developments in the field of electronics have been based solely on the charge current. Spintronics aims to improve the current technology by harnessing both charge and spin currents equally. It has been recognized, however, that it is quite a hard task to utilize spin currents unlike the case of charge currents. In this context, we have discovered new methods for generating spin currents.

Our method employs the spin transfer without charge transfer from a ferromagnet into an attached nonmagnetic conductor (metal or semiconductor), whose process is driven by the magnetization dynamics in the ferromagnet. When a magnetization in a ferromagnet is excited, it starts precession. Since a nonmagnetic conductor acts as a spin absorber, attaching a nonmagnetic conductor to the excited ferromagnet results in an emission of a certain amount of spins into the conductor as a result of the angular momentum conservation. Therefore, the spin current is generated in the nonmagnetic conductor without charge transfer across the interface of the ferromagnet/nonmagnetic conductor bilayers. This is a simple and versatile method because any perturbation exciting the magnetization dynamics enables this new type of spin current generation. We have demonstrated that this is indeed the case in the following ways.

First, we have shown that the spin current can be generated by sound waves. In a hybrid structure of a nonmagnetic metal (Pt) and an insulating ferromagnet ($Y_3Fe_5O_{12}$) as schematically shown in Fig. 1, a propagating sound wave is generated by a piezoelectric actuator attached to the ferromagnet. The sound wave then excites magnetization dynamics through the magneto-elastic coupling, thereby injects a spin current into the nonmagnetic metal. The spin current obtained is converted into an electric current via the spin-Hall effect. Thus, we have established a new route for generating spin and electric currents by ubiquitous sounds. This mechanism will be useful for constructing new spintronic and energy-saving devices.

Second, we have succeeded in injecting spin currents into semiconductors with a very high efficiency (10^3 times larger than before). So far, any attempt to generate spin currents in semiconductors has relied on the spin-polarized charge transfer from ferromagnets into semiconductors. However, the prevous attempts suffer from the so-called impedance mismatch problem arising from the extreme difference of the electric conductivity between ferromagnets and semiconductors. Using a hybrid structure of a semiconductor (GaAs) and a ferromagnet ($Ni_{81}Fe_{19}$) shown in Fig. 2 and by applying a microwave to the ferromagnet, we have shown that a high efficiency spin injection into GaAs is possible. This technique relies purely on the spin transfer caused by microwave-excited magnetization dynamics, and is free from the impedance mismatch problem that arises in the charge transfer. Since semiconductors are basic materials for conventional electronic devices, the impact of this finding on the spintronics community is astonishingly large.

A variety of such high-efficiency methods for spin current generation can make progress in spintronics, which in turn contributes to the development of energy-saving society as spintronics offers a route to reduce power consumption of solid-state logic devices.

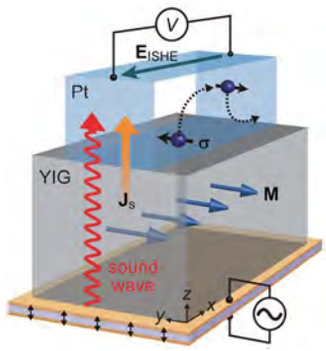

Fig. 1 Schematic illustration of the device structure to realize the new way of spin current generation by sound waves.

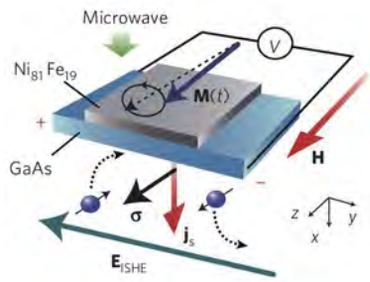

Fig. 2 Schematic illustration of the device structure to realize the new way of spin current generation by microwaves.

References

[1] K. Uchida *et al*., Nature Materials **10**, 737 (2011).
[2] K. Ando *et al*., Nature Materials **10**, 655 (2011).

Tailor-made graphene for spintronic and nanoelectronic applications

S. Entani, Y. Matsumoto, M. Ohtomo, P. V. Avramov, H. Naramoto, and S. Sakai
R. G. for Molecular Spintronics, ASRC, JAEA

Graphene proved interesting for nanoelectronics and spintronics. There have been plenty of attempts to fabricate graphene-based devices. To realize the spintronic and nanoelectronic devices using graphene, particular concerns should be addressed to the following two issues: The first one is to form the well-defined interface between graphene and metal electrodes. The elucidation and control of the injection/detection processes of spin-polarized carriers through the graphene/metal interface are essential for designing device properties [1]. The second one is to synthesize graphene film with large area and uniform number of carbon layer. The most conventional and commonly used fabrication method of graphene is the micromechanical exfoliation of graphite [2]. However, this process cannot satisfy above requests due to the following reasons: limited sizes with large distribution in shape and layer number as well as the contamination and impurities introduced during the fabrication process. Ultrahigh vacuum chemical vapour deposition (UHV-CVD) [3] can be a promising alternative method. The UHV-CVD growth makes it possible to prepare an epitaxial graphene film on the metal surface with large area and uniform layer-number of carbon sheet. In UHV-CVD, it is considered that graphene grows by the dissociation and polymerization of hydrocarbon molecules as precursors on the catalytic metal surfaces. This allows us to control the crystallinity by the growth condition.

In this study, the process of the UHV-CVD growth of graphene on Ni(111) thin films and with benzene as a precursor are investigated using *in-situ* reflection high energy electron diffraction (RHEED) and Auger electron spectroscopy (AES) [4]. Figure 1 shows changes in the RHEED specular beam intensity and the Auger intensity ratio, I_C/I_{Ni}, of the C *KLL* peak, I_C, and Ni *LMM* peak, I_{Ni} as a function of benzene exposure. It is successfully shown that SLG and bilayer graphene (BLG) can be synthesized by the control of benzene exposure in the range in $10-10^5$ langmuirs (L, 1 L = 10^{-6} Torr·sec) reflecting a change in the growth rate by three orders of magnitude in between the first and second graphene layer on the Ni(111) surface.

The electrical states of the transferred graphene sheets on the SiO_2 substrate are examined from the positions of the G peak and the 2D peak (Pos(G) and Pos(2D), respectively) in the Raman spectra. Figure 2 shows a plot of Pos(2D) *vs.* Pos(G) obtained from the randomly selected areas on the graphene sheets prepared with different benzene exposures and on the exfoliated SLG sheet. The linear increase of Pos(2D) with Pos(G) as seen in exfoliated SLG is reflective in the degree of hole doping, and the wide distribution of the peak positions, 1580−1592 cm^{-1} in Pos(G) and 2687−2704 cm^{-1} in Pos(2D), is due to the non-uniformity of the unintentional hole doping [1]. In case of the graphene sheets prepared by UHV-CVD, the Pos(G)-Pos(2D) relationship deviates from the linear one and there are rough tendencies to shift the G peak position to lower energy and the 2D peak position to higher energy with increasing exposure. These changes of the G and 2D peak positions with exposure are attributed to the increase of the layer number. As a striking feature, it is found that the distribution of Pos(G) and Pos(2D) becomes extremely small in SLG and BLG sheets (62 L and 1.1 × 10^5 L, respectively). These graphene sheets are presumed to be hole-doped judging from Pos(G) and Pos(2D) which are rather close to the linear relationship in the exfoliated SLG sheet. It can be said that the uniformity of the doping degrees in graphene can be improved remarkably by using UHV-CVD under the well-controlled exposure conditions instead of micromechanical exfoliation.

The present results demonstrate that the UHV-CVD method enables a tailor-made growth of graphene which would be necessary for controls of spin transport properties including realization of a long spin diffusion length in the graphene-based spintronicdevices beyond the limits of exfoliated graphene.

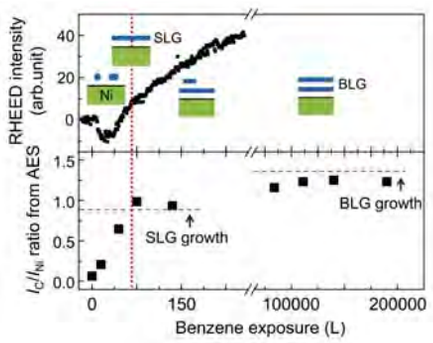

Fig. 1 (upper) Change in the RHEED specular intensities and (lower) plot of the AES intensity ratio, I_C/I_{Ni}, as a function of benzene exposure.

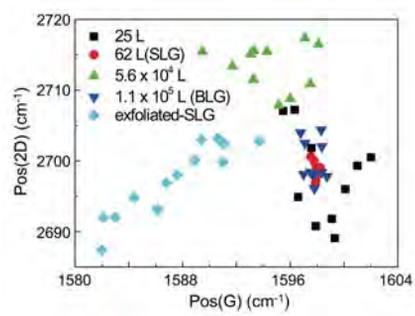

Fig. 2 Pos (2D) as a function of Pos (G). The symbols ■, ●, ▲, ▼ and ◆ denote the data obtained from the different areas on the graphene sheets prepared at 25 L, 62 L, 5.6 × 10^4 L, 1.1 × 10^5 L exposures and on the exfoliated SLG sheet, respectively.

References

[1] S. Entani *et al.*, J. Phys. Chem. C **122**, 345 (2010).
[2] K. S. Novoselov *et al.*, Proc. Natl. Acad. Sci. USA **102**, 10451 (2005).
[3] C. Oshima *et al.*, J. Phys. Condens. Mater. **9**, 1 (1997).
[4] S. Entani *et al.*, J. Appl. Phys. **111**, 064324 (2012).

First observation of ^{239}Pu NMR −A new frontier for the physics and chemistry of actinide compounds

H. Chudo[1,2], H. Yasuoka[1,2], G. Koutroulakis[2], S. Richmond[2], E. D. Bauer[2], J. D. Thompson[2], and D. L. Clark[2]
1) R.G. for Mechanical Control of Materials and Spin Systems, ASRC, JAEA
2) Los Alamos National Laboratory

We present here a success story of the first observation of ^{239}Pu Nuclear Magnetic Resonance (NMR) signal [1]. This finding puts an end to a fifty-year long search for Pu NMR, and opens new frontiers for the study of plutonium in the fields of solid state physics, chemistry, and nuclear materials science.

There are two main reasons why ^{239}Pu NMR has remained elusive. First and foremost, in atoms with unpaired f electrons, like rare earths and actinides, an extremely strong hyperfine interaction between electron and nuclear spins gives rise to a large internal magnetic field at the nuclear site. As a consequence, the resonance frequency is shifted by several orders of magnitude and the nuclear spin-lattice relaxation time (T_1) becomes exceedingly short, rendering any NMR measurement on Pu-based compounds very challenging. Secondly, there is no accurate account of the ^{239}Pu nuclear moment, hence neither of the relevant value of nuclear gyromagnetic ratio (gamma value).

In order to overcome above difficulties we have selected a compound in which Pu ion is in tetravalent state, and coordinated in a cubic local symmetry. The best material we have selected is PuO_2 where Pu ions should be Pu^{4+} ($5f^4$, $^3H_4$) and the ground state in a cubic crystalline filed is Γ_1 singlet. Since the magnetic excited state Γ_4 is located 123 meV higher in energy, the Pu^{4+} ion in PuO_2 should be almost nonmagnetic below room temperature. As for the problem of undetermined gamma value, we have just made use of the way of scanning external filed from the minimum to the maximum expected values at a constant frequency.

A high purity PuO_2 powder sample which was prepared by nitric and anion exchange follows by oxalate precipitation was used [2]. The ^{239}Pu abundance is about 94%, and 48.7 mg of powder PuO_2 was mixed 24 mg stycast epoxy and casted the sample with a Teflon mold. The typical sample dimensions were 1.5 × 1.5 × 9 mm^3. All our NMR experiments were performed using a superconducting, highhomogeneity, variable 8 Tesla magnet. The low temperature environment was provided by a standard Variable Temperature Insert ^{4}He flow cryostat. A bottom-tuned NMR probe was used, with variable tuning and matching capacitors mounted near the NMR coil allowing for wide frequency coverage. The data were recorded with a commercial NMR spectrometer. All experiments have been executed at Los Alamos National Laboratory (U.S.A.).

The first field-swept scan was made at 16.51 MHz and 3.95K. The external field was scanned from 3 T to 8 T to cover wide range of the gamma values with 0.06 T step. In this scan we have used t_{90} = 3 μs and t_{180} = 6 μs pulse width for exciting and refocusing RF pulses, respectively. The time duration between the first and the second pulse (τ) was 60 μsec and the repetition time of 1 s was used. In the Fig. 1(a), one can observe a clear spin-echo signal at 5.8 T. *This is the first observation of ^{239}Pu NMR signal.*

In order to determine the gamma value in PuO_2 precisely, the NMR spectrum has been measured at several deferent frequencies and a frequency−field diagram has been constructed. From a least-square fit of the slope, the gamma value in PuO_2 has been determined to be $^{239}\gamma_n(PuO_2)$ = 2.856 ± 0.001 MHz/T.

We have tried to obtain the value of T_1 using the inversion recovery method. As is expected from the singlet ground state of Pu^{4+}, the T_1 value is expected to be extremely long at low temperatures. Actually, we could not obtain the correct value of T_1 by the inversion recovery method. Nevertheless, we could place the best estimate of 100 s at 4 K. This long T_1 assures that the observed NMR is really associated with Pu^{4+} in PuO_2.

The gamma value obtained here is exclusively for the case of ^{239}Pu in PuO_2 and it is not necessarily the "bare" gamma value of ^{239}Pu. In order to estimate bare gamma value, we have used the free ion value of the hyperfine coupling constant A_{hf} = 283.5 T/μ_B [3] to estimate the value of NMR shift (K) in PuO_2. Combined with the susceptibility data, χ_o=5.36×10^{-4} emu/mol, K is obtained to be +24.8% using a relation of K= ($\chi_o \cdot A_{hf}$) /($N_A \cdot \mu_B$). Since the bare gamma vale γ_n is expressed as $^{239}\gamma_n$= $^{239}\gamma(PuO_2)$/(1+K), we have the value of 2.29 MHz/T, corresponding to a nuclear moment of 0.15 μ_N for ^{239}Pu.

We also performed measurements on a sample known to be not fully oxidized, i.e., PuO_{2-x}. In Fig. 1(b) a ^{239}Pu NMR spectrum is shown, taken by sweeping the external magnetic field (Ho= 4.45 − 5.05 T) at f = 12.1 MHz and T = 4 K. The spectrum consists of two lines with NMR shifts K ≈ 11% and K ≈ 19%, respectively. Although we do not have a firm conclusion, we infer that those lines are associated with either Pu atoms nearby oxygen vacancies in PuO_{2-x} or Pu atoms in an α-Pu_2O_3 impurity phase. Controlled experiments are necessary for a definitive conclusion; nevertheless, this observation assures that the Pu NMR spectrum is sensitive to the oxygen coordination and can provide an atomic-scale fingerprint of the oxidation process. This is of particular importance for understanding the consequences of long-term storage of plutonium.

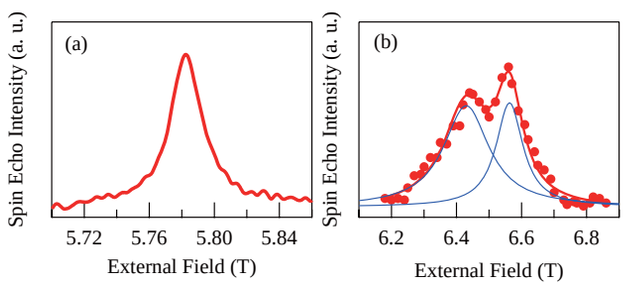

Fig. 1 ^{239}Pu NMR (Spin-echo) field swept spectra taken at 16.51 MHz and 3.95 K. (a): Pure PuO_2, (b) Nonstoichiometric PuO_{2-x}.

References

[1] H. Yasuoka, H. Chudo *et al*., Science **336**, 901 (2012).
[2] Materials and Methods are available as supplementary material in *Science Online*.
[3] B. D. Dunlap *et al*., in Actindes, (Academic Press, New York, 1974), **1**, p. 237 and references therein.
[4] G. Raphael *et al*., Solid State Communications **6**, 383 (1968).

Anomalous electrical resistivity associated with unconventional superconductivity in URu_2Si_2

N. Tateiwa[1)], Y. Haga[1)], T. D. Matsuda[1)], Y. Onuki[2)], and Z. Fisk[1, 3)]
1) R.G. for Actinide Materials, ASRC, JAEA
2) Osaka University 3) University of California

Unconventional superconductivity (SC) in the uranium compound URu_2Si_2 below T_{sc} = 1.4 K has attracted much attention due to its novel superconducting properties [1]. The SC has a strong relation with the electronic state of an unknown ordered phase whose transition temperature is T_0 = 17.5 K at ambient pressure. The nature of the ordered phase known as "hidden order" (HO) has not been resolved for more than 25 years. The low temperature physical properties of URu_2Si_2 are very sensitive to the sample quality. We have grown a high quality single crystal of URu_2Si_2 to eliminate impurity effects [2]. In this study, we have investigated the electrical transport under high pressures [3].

Figure 1 shows the pressure-temperature phase diagram in URu_2Si_2 [3]. The ground state is changed from the HO to the antiferromagnetic (AF) state at a first order phase transition pressure P_x. The bulk superconducting state exists only below P_x. We have measured the electrical resistivity ρ under high pressure. The electronic property of the ordered state is reflected through the scattering process of electron. For example, the usual electron-electron scattering gives the T^2-term in the resistivity. We focus on the pressure effects on T_{sc} and the electrical transport. We analyse the temperature dependence of ρ using the expression $\rho = \rho_0 + \alpha_1 T + \alpha_2 T^2$, assuming that the resistivity ρ consists of a T-linear resistivity from the unusual scattering process of electron and the usual T^2-term.

We find a linearity between α_1/α_2 and T_{sc} as shown in Fig. 2. The pressure dependence of the coefficient of α_2 is very weak. The value of T_{sc} depends primarily on the coefficient α_1. This suggests that the anomalous electron scattering derives the unconventional SC in the hidden order phase. This finding provides a key for further studies on the hidden and SC states in URu_2Si_2 [3].

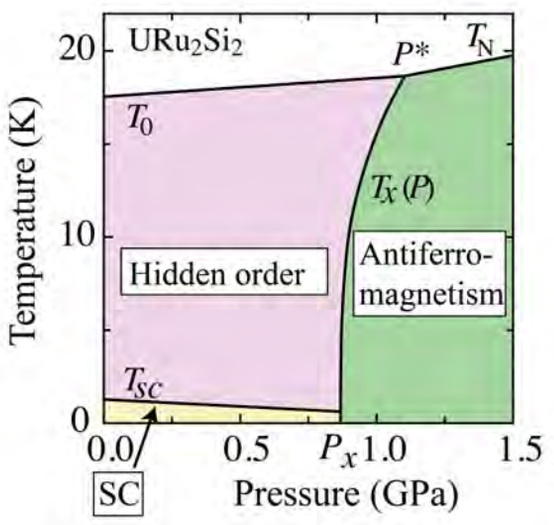

Fig. 1 Temperature pressure phase diagram in URu_2Si_2. "SC" indicates the superconducting phase.

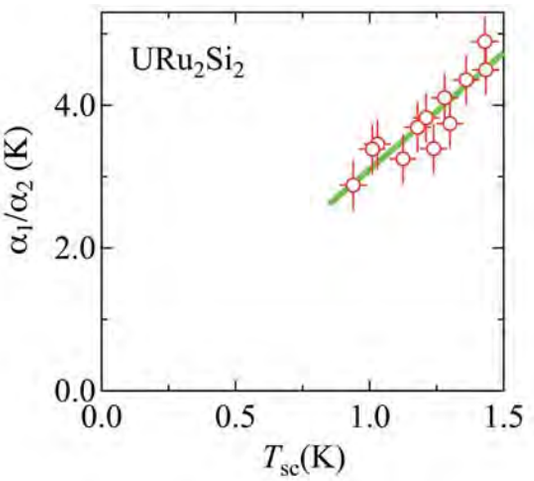

Fig. 2 Relation between α_1/α_2 for the resistivity ρ and superconducting transition temperatures T_{sc}, where the α_1 and α_2 are obtained by the fitting to $\rho_0+\alpha_1 T+\alpha_2 T^2$.

Similar correlation between the T-linear resistivity and T_{sc} has been found in the organic superconductors, the iron pnictide superconductors and the high-T_c cuprate superconductors [4]. This correlation may be a universality in the unconventional superconductors. In these systems, the T-linear resistivity appearing around a magnetic phase boundary has been interpreted as manifestation of quantum criticality.

So far, many theoretical models have been proposed for the HO phase. Generally, the peculiarity of the HO phase originating from the multipolar degree of freedom in the 5f electrons has been stressed but no clear experimental evidence was found. Unidentified mysterious phases have been reported near the SC phase such as "pseudo-gap phase" in the cuprate superconductors. We note recent studies on the mysterious phases from the view point of electronic nematicity [5]. Interestingly, the symmetry breaking of the electronic state has been revealed also in the HO phase by the collaboration work between our research group and Kyoto University [6]. The result as well as the present finding suggests that the HO phase in URu_2Si_2 shares the universality inherent to the strongly correlated electron superconductors near quantum criticality. Our studies provide a different point of view for theories of the HO phase. Future studies on the phase will contribute to the understanding of all strongly correlated electron systems.

References

[1] T. T. M. Palstra *et al.*, Phys. Rev. Lett. **55**, 2727 (1985).
[2] T. D. Matsuda *et al.*, J. Phys. Soc. Jpn. **80**, 114710 (2011).
[3] N. Tateiwa *et al.*, Phys. Rev. B **85**, 054516 (2012).
[4] L. Taillefer, Annu. Rev. Condensed Matter Phys. **1**, 51 (2010).
[5] J-H. Chu *et al.*, Science **329**, 824 (2010).
[6] R. Okazaki *et al.*, Science **331**, 439 (2011).

Magnetic-field-induced quantum critical behavior in the heavy-fermion superconductor $CeCoIn_5$: ^{59}Co Nuclear Magnetic Resonance study

H. Sakai[1,3], S. E. Brown[2,3], S.-H. Baek[3], F. Ronning[3], E. D. Bauer[3], and J. D. Thompson[3]
1) R. G. for Condensed Matter Physics of Heavy Element Systems, ASRC, JAEA
2) University of California 3) Los Alamos National Laboratory

The need to determine the nature of spin fluctuations and their possible relationship to unconventional superconductivity in heavy fermion systems, and strongly correlated systems more broadly, has posed a long-standing problem. The intermetallic compound $CeCoIn_5$ with a tetragonal crystal structure is an absolutely fascinating material. The superconducting critical temperature T_c for this compound is 2.3 K, which is the highest among Ce-based heavy fermion systems. Moreover, it exhibits the various physical phenomena such as heavy fermion behavior (i.e. large electronic specific heat coefficient $\gamma \sim 1000$ mJ mol^{-1} K^{-2}), anisotropic superconductivity, magnetic-field-induced spatially-modulation of superconductivity with coexistence of antiferromagnetism (this is animatedly discussed if it may be Fulde-Ferrell-Larkin-Ovchinnikov (FFLO) state), quantum criticality and so on. These rich physical properties in $CeCoIn_5$ are thought to occur in the background of strong antiferromagnetic correlations. Nuclear magnetic resonance (NMR) technique is one of the most suitable tools to evaluate such spin dynamics microscopically, while the usual transport measurements cannot estimate it directly. We have preformed the ^{59}Co-NMR measurements for $CeCoIn_5$ as functions of external magnetic fields (H_0) and temperatures (T), in order to evaluate how the antiferromagnetic spin fluctuations develop toward the anisotropic superconductivity at the lowest temperatures. Since the perturbation energy is quite small of $\sim 10^{-5}$–10^{-2} meV in NMR spectroscopy, NMR relaxation rate $1/T_1$ responds promptly to the dynamical susceptibility of the electronic states. In general, NMR $1/T_1$ corresponds to the square of hyperfine coupling constant (A_{hf}^2) times $\Sigma_q \mathrm{Im}\chi(\boldsymbol{q}, \omega)$, the latter of which is the imaginary part of momentum space ($\boldsymbol{q}$)-summed electronic dynamical susceptibility. Although A_{hf} is usually T-independent, the A_{hf} for ^{59}Co nuclei in $CeCoIn_5$ has been found to be T-dependent for ^{59}Co from our previous work [1]. This T-dependent $A_{hf}(T)$ has been used for the successive detailed analyses based on the uniform dynamical susceptibility by Ce 4f electrons. For example, in the case of normal metal (i.e. Fermi-liquid state), $(T_1T)^{-1}/A_{hf}^2$ is known to become constant, and its constant value corresponds to the enhancement of electronic correlations.

In the case of H_0 well above the superconducting critical field $H_{c2}(0) \sim 5$ T parallel to the c-axis (see the 8 T data in Fig. 1), the normalized $(T_1T)^{-1}/A_{hf}^2(T)$ shows a constant value in the lowest temperatures below ~1 K. As the external fields decreases toward to 5 T, $(T_1T)^{-1}/A_{hf}^2(T)$ shows a critical increase in the lowest temperatures [2]. As shown in Fig. 1, this critical behavior of $1/T_1$ is well explained by the theoretical model of antiferromagnetic spin fluctuations, i.e. self-consistent renormalization (SCR) theory, which has been applied successfully to characterize the nature of spin fluctuations in many heavy fermion materials [3]. In addition, it is found that the obtained parameters from the fit to $1/T_1$-data can explain the H_0-dependence of macroscopic physical properties such as resistivity, specific heat, and thermal expansion in the same theoretical framework.

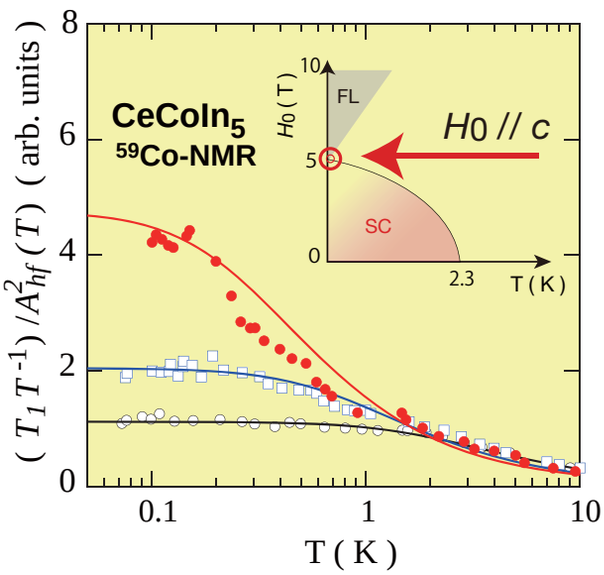

Fig. 1 T-dependence of the normalized $(T_1T)^{-1}/A_{hf}^2(T)$ for ^{59}Co-NMR in $CeCoIn_5$ under the external fields of 8, 6.4, and 5 T parallel to c-axis. The solid curves represent the calculated curves based on the theoretical model of antiferromagnetic spin fluctuations [2]. The inset shows the schematic H_0-T phase diagram in the case of H_0 parallel to the c-axis.

Thus, our results have conclusively proved that the quantum critical behavior near $H_{c2}(0)$ for the heavy fermion superconductor $CeCoIn_5$ is caused by the antiferromagnetic spin fluctuations. Such kind of field-tuned criticality may exist even in the high-T_c cuprates, in which antiferromagnetic spin fluctuations develop well, although it cannot be verified easily since the $H_{c2}(0)$ for these superconductors is extensively higher. Perhaps, this work may provide small-scale, but really identifiable values for building a new theory to design for a new higher-T_c material.

References

[1] H. Sakai *et al.*, Phys. Rev. B **82**, 020501(R) (2010).
[2] H. Sakai *et al.*, Phys. Rev. Lett. **107**, 137001 (2011).
[3] S. Kambe *et al.*, J. Low Temp. Phys. **108**, 383 (1997).

Local distributions of radioactive Cs deposited on plant and soil from Fukushima Daiichi Nuclear Power Plants

F. Sakamoto[1)], T. Ohnuki[1)], N. Kozai[1)], S. Igarashi[1,2)], S. Yamasaki[1)], Z. Yoshida[3)], and S. Tanaka[4)]
1) R. G. for Bioactinide, ASRC, JAEA 2) Ibaraki University 3) JAEA
4) NPO Radiation Safety Forum

After the accident of Fukushima Daiichi Nuclear Power Plant (FDNPP), the fallout radioactive Cs were dispersed from FDNPP to ocean [1,2] and land [1]. Some of the released radioactive Cs was deposited on the ground of the area located north-west direction from FDNPP. The spatial concentration distribution and depth profiles of radioactive Cs were measured to estimate dose rate and to estimate the fate in the terrestrial environment.

For the estimation of migration of radioactive Cs, chemical states of the deposited radioactive Cs should be clarified. We first sampled the soils, plants, and paddy area at Iitate-mura, Fukushima on June, 2011 to estimate the chemical states of radioactive Cs deposited [3]. We have measured local distribution on/in trees, plants, and surface soil beneath the plants using autoradiography analysis.

The trees sampled were *Cryptomeria japonica*, *Torreya nucifera*, and *Prunus mume*. The grass at meadow area and rice (*Orysa sative*) stubble at paddy area were collected with soil attached around roots. The local distribution of radioactive Cs was measured by autoradiography technique using Bioimaging analyzer of BAS2500 (Fuji Film, Japan). The samples were not pretreated for the autoradiography analysis. The shape and color of the samples were recorded by optical photograph.

The autoradiography images of *Torreya nucifera* is shown in Fig. 1 along with optical photograph. The black points in the autoradiograph image showed the area of radioactive Cs was accumulated. The black spots sized about 2 mm were distributed on the branch and leaves of *Torreya nucifera*, indicating that radioactive Cs was distributed heterogeneously on the branch and leaves of trees. The area of red circles in Fig. 1 showed no black spot on the branch and the leaves. The optical photograph showed that the color of the leaves in the red circles sickly green. This indicates that the branch and leaves in the red circles were grown in this year probably after the FDNPP accident. These results suggest that only small fraction of deposited Cs may be transported to new branch and leaves grown after the accident. Little fraction of the deposited radioactive Cs was transported from the grown branch and leaves to new born ones. Similar results were obtained for *Cryptomeria japonica* and *Prunus mume*. By the treatment of the branch and leaves with a 1 M CH_3COOH solution showed approximately 5% of the radioactive Cs was dissolved from the branch and leaves into the acetic acid solution, indicating that radioactive Cs was tightly associated with the branch and leaves.

The autoradiograph image of grass at the meadow (Fig. 2) indicated the black spots were distributed on the grass above the ground level (yellow dashed line), but not with soil root beneath the ground level (red circles). The black spots on the stubble of rice showed similar distribution. These results indicated that the radioactive Cs was deposited on the grass and the rice plant. In addition, the ratio of the radioactive Cs penetrated into soil layer by weathering was very small for two months after accident. These results indicate that trees and plant would be the reservoir of the fallout Cs and function for retardation of the fallout Cs migration with rain water.

Fig. 1 Autoradiograph image (a) and optical photograph (b) of *Torreya nucifera* sampled at Iitate, Fukushima, about 30 km from FDNPP.

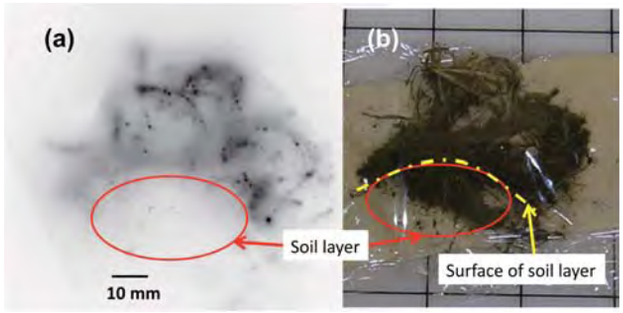

Fig. 2 Autoradiograph image (a) and optical photograph (b) of cross section of meadow grass with soil beneath the grass.

References

[1] M. Chino *et al.*, J. Nucl. Sci. Technol. **48**, 1129 (2011).
[2] A. Omoto, Prog. ICAPP2011 Special Japan Session: presentation (2-6 May, 2011, Nice, France).
[3] F. Sakamoto *et al.*, Trans. Atomic Energy Soc. Japan, **11**, 1 (2012) (*in Japanese*).

Li (Zn,Mn) As as a new generation ferromagnet based on a I-II-V semiconductor [REIMEI project]

Z. Deng[1)], C.Q. Jin[1)], Q.Q. Liu[1)], X.C. Wang[1)], J.L. Zhu[1)], S. M. Feng[1)], L.C. Chen[1)], R.C. Yu[1)], C. Arguello[2)], T. Goko[2)], Fanlong Ning[2,3)], Jinsong Zhang[4)], Yayu Wang[4)], A.A. Aczel[5)], T. Munsie[5)], T.J. Williams[5)], G.M. Luke[5)], T. Imai[5)], T. Kakeshita[6)], S. Uchida[6)], W. Higemoto[7)], T.U. Ito[7)], Bo Gu[8,9)], S. Maekawa[8,9)], G. Morris[10)], W.Q. Yu[11)], and Y. J. Uemura[2)]

1) IOP, Beijing 2) Columbia University 3) Zhejian University 4) Tsinghua University 5) McMaster University 6) University of Tokyo 7) R. G. for Condensed Matter Physics of Heavy Element Systems, ASRC, JAEA 8)R. G. for Condensed Matter Theory, ASRC, JAEA 9) CREST, JST 10)TRIUMF 11) Renmin University

Ferromagnetic systems obtained by doping transition metals into semiconductors [1] have generated extensive studies since early 1990's [2] because of their potential use for spin-sensitive electronics (spintronics) devices. In prototypical systems based on III-V semiconductors, such as (Ga,Mn) As and (In,Mn) As, substitution of divalent Mn atoms into trivalent Ga or In sites leads to severely limited chemical solubility, resulting in chemically metastable specimens available only as thin films [1]. Their materials quality exhibits high sensitivity on preparation methods [3], and self-doping of hole carriers via substitution prohibits electron doping. To overcome these difficulties, Masek *et al*. [4] theoretically proposed systems based on a I-II-V semiconductor LiZnAs, where magnetism due to isovalent (Zn,Mn) substitution may be decoupled from carrier doping with excess/deficient Li concentrations.

Recently we succeeded in synthesizing bulk poly-crystal specimens of $Li_{1+y}(Zn_{1-x}Mn_x)$ As and $Li_{1+y}(Cd_{1-x}Mn_x)$P at the Institute of Physics (IOP) of Beijing [5]. As shown in Fig. 1 for Li (Zn, Mn) As, these systems exhibit ferromagnetism with T_c up to 50 K in nominally Li-excess (y = 0.05–0.2) compounds with Mn concentrations x = 0.03−0.15, and a very low coercive field (30−100 Oe) promising for spin manipulations. Resistivity show metallic conductivity for Li deficient and Li excess systems. The Hall resistivity exhibits anomalous Hall term due to spontaneous magnetization, and, to our surprise, p-type carriers in Li excess systems. This is likely due to excess Li substituting the Zn or Cd site and forming an acceptor.

We performed MuSR measurements in $Li_{1.1}(Zn_{0.95}Mn_{0.05})As$, and confirmed static magnetic order below T_c ~ 27 K, with the full volume fraction at T = 0 [5]. In a plot of the muon spin relaxation rate (which represent the ordered moment size times concentration) and T_c, the results from Li (Zn,Mn) As and (Ga,Mn) As [6] exhibit a common slope, which suggests a common ferromagnetic interactions. These results are consistent with Local Density Approximation and quantum Monte-Carlo calculations by Gu and Maekawa.

The availability of bulk specimens allowed NMR studies in these two systems with signals from ^{7}Li and ^{31}P nuclei. The Li NMR in Li (Zn,Mn) As exhibits sharp peaking of the relaxation rate $1/T_1$ at the ferromagnetic transition temperature T_C. The observed scaling of $1/T_1T$ with $1/(T+T_W)$, appearing with a positive T_W in a wide temperature region above T_C, suggests an influence of antiferromagnetic coupling between Mn moments located in nearest-neighbor geometry.

As shown in Fig. 2, ferromagnetic Li (Zn,Mn) As (T_C ~ 50 K) and semiconducting LiZnAs have a crystal structure similar to those of antiferromagnetic LiMnAs (T_N ~ 450 K) and superconducting LiFeAs (T_c ~ 25 K), having common square-lattice As layers with 10% lattice constants matching. This feature may enable fabrication of junction devices of various combinations of these systems for spin-sensitive electronics.

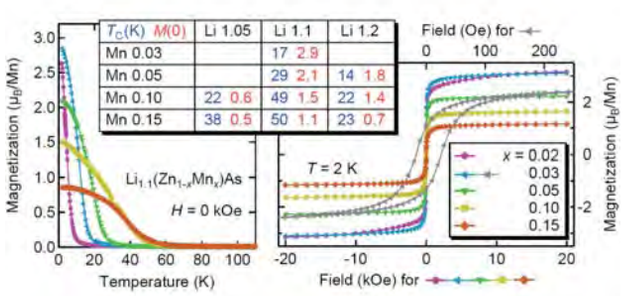

Fig. 1 Magnetization M (H) of $Li_{1.1}$ ($Zn_{1-x}Mn_x$) As. The gray symbol shows in a very small coercive field of 30-100 Oe. The inset table shows the values of T_c and the average ferromagnetic ordered moment size M (T=2K;H=2kOe) per Mn derived from magnetization measurements for nominally Li excess systems. (cited from [5])

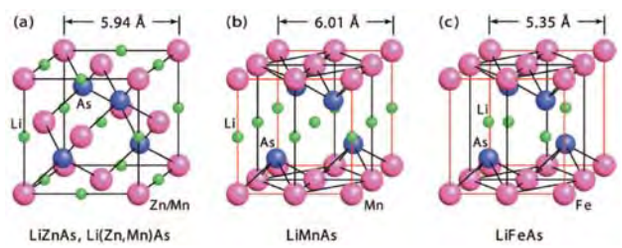

Fig. 2 Crystal structures of Li(Zn,Mn)As, LiMnAs and LiFeAs.

References

[1] H. Ohno, Science **281** ,951-956 (1998).
[2] T. Dietl, Nature Materials **9**, 965-974 (2010).
[3] S.J. Potashnik *et al*., Appl. Phys. Lett. **79**, 1495 (2001).
[4] J. Masek *et al*., Phys. Rev. Lett. **98**, 067202 (2007).
[5] Z. Deng *et al*., Nature Communications, **2**, 422 (2011) and in preparation.
[6] S.R. Dunsiger *et al*., Nature Materials **9**, 299-303 (2010).

Research Group for Condensed Matter Theory

Group Leader : Michiyasu Mori
Members : Hiroaki Onishi, Katsunori Kubo, Jun'ichi Ieda, Hiroto Adachi, Bo Gu, Mari Matsuo, Mamoru Matsuo, Yuta Yamane, Yuichi Ohnuma

We study new functional materials emerging from the electrons internal degrees of freedom (spin, charge and orbital) and the electrons correlation. New principle and new function of devices are also our important targets. So far, we have found (1) a new method of spin injection into all types of materials and (2) a spin current generation by a mechanical vibration (phonon). Details of these two results are summarized in Research Highlights. Studies on spin Seebeck effect, spin current generation by mechanical rotation, ferromagnetic Josephson junction with magnetic domain wall, and enhanced spin Hall effect are also progressing soundly.

Theory of spinmotive force and its continuous generation by highly asymmetric geometry

A spin-originated motive force, i.e., "spinmotive force", is the conversion of the magnetic energy in a ferromagnet into the electrical energy of conduction electrons via the magnetic exchange interaction. The spinmotive force is given by the spin electric field,

$$E_s = -\frac{P\hbar}{2e} m \cdot (\partial_t m \times \nabla m),$$

where m is the local magnetization, P is the spin polarization of conduction electrons. The Planck constant and the elementary charge are denoted by $\hbar$ and e, respectively. Note that both the time and the spatial variations of m are necessary to obtain the spinmotive force. So far, a motion of magnetization or ferromagnetic nano-particles has been used to generate the spinmotive force. Hence, the obtained results are limited to a pulse or ac-type generations.

We proposed a new method to generate a dc spinmotive force [1]. By exciting a ferromagnetic resonance in a comb-shaped ferromagnetic thin film as shown in Fig. 1, it is found that the continuous spinmotive force can be obtained. The spin electric field in the comb-shaped ferromagnet is calculated by supposing that the local magnetization dynamics is determined by the Landau-Lifshitz-Gilbert equation. Experimental results are quantitatively well reproduced by our theoretical calculations. Our theory can provide a microscopic understanding of the spinmotive force.

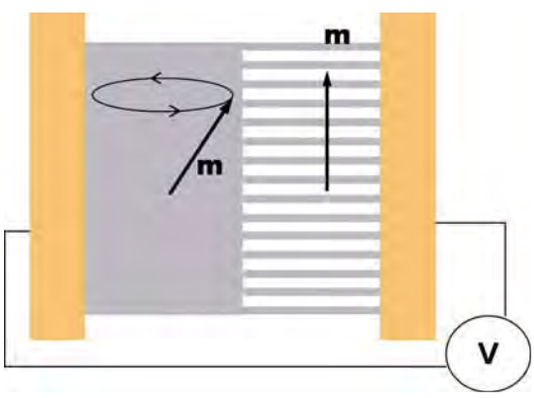

Fig. 1 Schematic of the comb-shaped ferromagnetic thin film. The ferromagnetic resonance frequency in the pad region (left) is different from that in the wire region (right).

Non-monotonic temperature dependence of thermopower in correlated electron systems

Since the discovery of unusually large thermopower in Na_xCoO_2, transition-metal oxides with strong electron correlation have attracted much attention as promising candidates for high-performance thermoelectric materials. Thermopower is none other than the amount of entropy flow along with the electric current. The consideration on the entropy in thermodynamics tells us the low and high temperature (T) limits of the thermopower: In the metallic systems, the thermopower goes to zero as T goes to 0 K. On the other hand, the high-temperature limit of thermopower is given by the entropy consideration in the atomic limit. In the strongly correlated systems, the spin and orbital degrees of freedom can enhance the high-temperature thermopower in principle.

We studied the role of strong Coulomb interaction on thermopower, whose temperature dependence is particularly examined in detail. For this purpose, the single- and multi-band Hubbard models are adopted as a minimum model and the strong Coulomb interaction is treated in the dynamical mean field theory (DMFT), which can capture the coherent-to-incoherent crossover due to the strong Coulomb interaction, U. This method based on the local picture is useful to understand the overall behavior of thermopower as a function of temperature. It is found that the Coulomb interaction gives rise to a non-monotonic temperature-dependence, which is well described by the entropy consideration at high temperatures. In the light of our theoretical results, the thermoelectric response in the transition metal oxides, $La_{1-x}Sr_xVO_3$ is well explained.

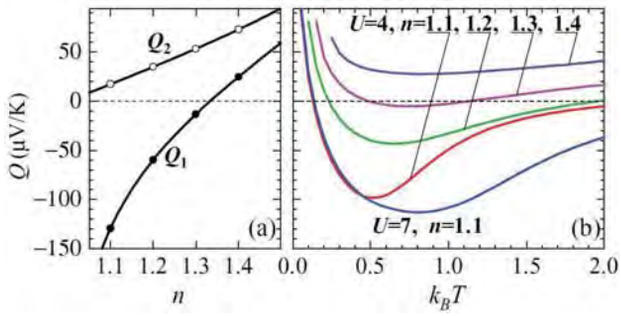

Fig. 2 (a) Thermopower in the high temperature limit, Q_1 ($T \to \infty$ with $k_BT<U$) and Q_2 ($T \to \infty$ with $U<k_BT$), vs. electron density, n in the single band Hubbard model. (b) Temperature dependence of the thermopower calculated by DMFT with the non-crossing approximation as impurity solver, for various parameter sets of U and n.

References

[1] Y. Yamane *et al.*, Phys. Rev. Lett. **107**, 236602 (2011).
[2] M. Uchida *et al.*, Phys. Rev. B **83**, 165127 (2011).
[3] M. Matsuo *et al.*, Phys. Rev. B **84**, 153107 (2011).

Research Group for Molecular Spintronics

Group Leader: Seiji Sakai
Members: Yoshihito Matsumoto, Shiro Entani, Manabu Ohtomo, Pavel V. Avramov

Spintronics is an emerging technology taking advantage of the dual freedom of both charge and spin degrees. Since the discovery of the giant magnetoresistance of metal multilayers in 1988 (A. Fert and P. Grünberg, the 2007 Nobel Prize in Physics), spintronics has been developed based on inorganic substances like metals and semiconductors. Recent studies have started to shed light on spintronic applications of molecular materials including organic molecules and nanocarbons in which the spins of conduction electrons can be preserved for a long time and distance. We call this new field "Molecular spintroncis".

In molecular spintronics, efficient control of spin transport processes (spin injection, manipulation and detection) in molecular materials are of special importance to realize spintronic applications. Our group aims at elucidating the advantages of molecular materials as innovative spintronic materials by exploring novel systems for efficient spin transport control based on the hybrid systems of molecular materials and magnetic metals and also by developing cutting-edge spectroscopy techniques for the electronic and magnetic states of the molecular material-based structures and interfaces therein. Typical progresses in FY2011 are summarized in the following.

Precise layer number control of graphene in ultra-high vacuum chemical vapour deposition

After the discovery of the convenient fabrication method by the exfoliation from graphite (A. Geim and K. Novoselov, the 2010 Nobel Prize in physics), graphene has been attracting world-wide attention as an innovative electronic material. In the spintronics, graphene is expected to be an ideal spin-transport material due to the extremely long spin diffusion length and high carrier mobility. However, not only the non-uniformity in the carbon layer number and in the electronic states but also the polycrystalline nature of exfoliated graphene are making it impossible to control the spin transport properties in graphene. It can be said that a new fabrication method which enables tailoring of graphene is necessary for the development of spintronic applications.

From the above view point, ultrahigh vacuum chemical vapor deposition (UHV-CVD) can be an alternative fabrication method, because single-layer graphene is known to be epitaxially grown on the catalytic metal crystal. In UHV-CVD, graphene grows through the dissociation and polymerization of hydrocarbon precursors on the metal surfaces.

In this study [1], we focused on a UHV-CVD growth of microstructure-controlled graphene by using epitaxial metal thin films as a catalytic substrate and with *in-situ* spectroscopy. It was successfully demonstrated that single-crystalline graphene (single-layer and bilayer graphene) with the same number of carbon layer over the entire area can be obtained by precise control of the exposure amount of precursors. In addition, it was suggested that the uniformity of the electronic states in UHV-CVD graphene can be remarkably high compared to exfoliated graphene (see the Research Highlight for additional details).

Our findings would enable controls of spin transport properties of graphene and lead to the development of graphene-based spintronics and nano-electronics.

Very high interface spin polarization and its mechanism in fullerene-magnetic metal system

Generation of high spin polarization of conduction electrons at the interface between the magnetic electrode and molecular transport medium is essential for efficient spin injection. After 1988, magnetic metal crystals have been commonly used for a magnetic electrode in spintronic devices. However, it has been pointed out that much higher spin polarization than that in magnetic metal crystals or an appropriate barrier material is necessary to realize high spin injection efficiency overcoming the conductivity mismatch problem that can limit spin polarization of injected electrons into a molecular medium [2].

In this study, it was demonstrated that new compounds of fullerene and magnetic metal (e.g., C_{60}-Co compound, see Fig. 1) can be a promising barrier material which gives rise to nearly-complete spin polarization of conduction electrons at the interface with magnetic metal crystals. In order to elucidate the magnitude of spin polarization at the interface with the magnetic metal crystal, the characteristics of tunnelling current and magnetoresistance were analysed for the C_{60}-Co films consisting of a C_{60}-Co compound and a small amount of Co nanocrystals [3, 4]. It was revealed that spin polarization increases as high as 80% at the C_{60}-Co compound/Co crystal interface in comparison with that in Co crystal (30%). Our theoretical analysis [5] based on the X-ray absorption and magnetic circular dichroism spectroscopy indicated that the C_{60}-Co compound can work as a spin filtering barrier due to the exchange splitting in the LUMO region as represented in Fig. 1.

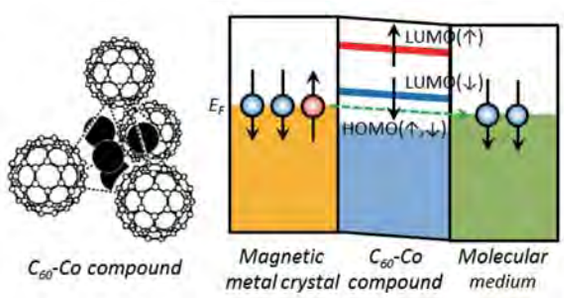

Fig. 1 Atomic structure of the C_{60}-Co compound (left) and a schematic view of the spin filtering effect of the C_{60}-Co compound as a tunnelling barrier for spin injection into a molecular medium (right) [5, 6]. LUMO/HOMO and up/down arrows in the right figure represent the lowest unoccupied/highest occupied molecular orbital and up/down spin, respectively. The HOMO-LUMO (band) gaps in the C_{60}-Co compound are smaller for the spin-down electrons (0.8 eV) than that for the spin-up electrons (1.9 eV), which causes spin filtering.

References

[1] S. Entani *et al.*, J. Appl. Phys. **111**, 064324 (2012).
[2] G. Schmidt *et al.*, Phys Rev. B **62**, R4790 (2000).
[3] S. Sakai *et al.*, Phys. Rev. B **83**, 174422 (2011).
[4] S. Sakai *et al.*, J. Magn. Magn. Mater. **324**, 1970 (2012).
[5] I. Hojo *et al.*, J. Electro. Spec. Relat. Phenom. **185**, 32 (2012).
[6] A. Nakajima *et al.*, J. Phys. Chem. A **104**, 176 (2000).

Research Group for Mechanical Control of Materials and Spin Systems

Group Leader : Eiji Saitoh
Members : Satoru Okayasu, Masao Ono, Rie Haruki, Hiroyuki Chudo, Hiroshi Yasuoka

The research objective of our group is to develop new methods for controlling spin currents by combining electron spins and mechanical rotation, and/or by coupling spins and NMR techniques. That is to expand spintronics frontier using mechanical motion and NMR method. Our goals are :

1) Magnetization manipulation in terms of mechanical rotation.
2) Detection of a spin current generated from rotating objects using the spin Hall and spin torque effect.
3) Detection of spin transfer between nonmagnetic and ferromagnetic layers by NMR.

Ferrromagentic enhancement in Barnett effects measured with a highly stabilized rotator at high temperatures

To overcome the difficulty of detecting the tiny effective magnetic fields induced by rotations, improvements of the high-speed rotation system are needed for the reduction of the magnitude of environmental fields. The residual magnetic field less than 10 mOe has been achieved by improving the electromagnetic shielding of the system. Figure 1 is a plot of magnetizations of a ferrite sample after a series of experiments for observing the Barnett effect. The sample is cooled after heating to 500 (above the Curie temperature 480) with or without the rotations. Squares are the magnetization of the sample without the rotations, and circules are those with the rotations where the rotational speed is 0.5 kHz. We observed the systematic shifts of the magnetization by rotation (Fig. 1). This implies that the effective magnetic field induced by the rotations modulates the net magnetization, consistent with the Barnett effect affected by the magnetic transition instability

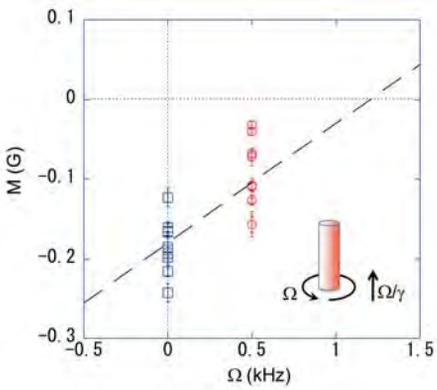

Fig. 1 Magnetization of a sample by rotations with the angular speed of Ω.The dotted line represents $M=\chi(\Omega/\gamma+H_{env.})$. Sample: anisotropic ferrite magnet with the dimension of 5 mm long and φ1 mm in diameter, $H_{env.} = -0.01$ Oe.

Spin pumping induced by the FNR in a Pt/Co_2MnSi hetero junction

Transfer of spin angular momentum from a precessing localized spin to the conduction electron is called the spin pumping. The spin pumping from ferromagnetic magnetization has already been established, and it has been used as a basic technique for the spin current generation. However, the microscopic mechanism has not been elucidated yet, particularly underlying physics of the interface spin exchanges. In order to take further steps to understand the phenomena, we have been trying to generate a spin current using the spin pumping from resonating nuclear spins. An experimental strategy in this category is rather simple; we have tried to detect a current in the nonmagnetic metallic layer attached to a ferromagnetic layer via the inverse spin Hall Effect (ISHE) which converts a spin current into an electric current. Here the spin pumping is driven by ferromagnetic nuclear resonance (FNR) which coupled strongly to the magnetic moment of electrons via the hyperfine coupling in the order of 10-100 T/μ_B. The ferromagnetic layer used in the present study was Heusler compounds Co_2MnSi, because it contains ^{59}Co and ^{55}Mn nuclei whose natural abundances are 100%, being appropriate for FNR. A spin current generated by the spin pumping that is driven either by the ^{59}Co and ^{55}Mn FNR is detected by the ISHE in the Pt layer.

Figure 2(a) shows the schematic illustration of the setup for the measurement of spin pumping using ^{59}Co and ^{55}Mn FNR. The sample is an array of Pt(7 nm)/Co_2MnSi(20 nm) thin rectangular films with width of 0.8×9 mm^2 in size. These films were wired in series fashion in order to obtain the amplified voltage arising from the ISHE. The sample assembly was inserted into an RF-coil, where the RF field for FNR was applied parallel to the electrodes on the Pt layer. In order to align the ferromagnetic domains, 270 Oe fields were applied within the film plane and were rotated with respect to the direction of the RF field. The FNR spectra associated with the ^{59}Co and ^{55}Mn nuclei in Pt(7 nm)/Co_2MnSi(20 nm) are shown in Fig. 2(b). The fractional change in the voltage across the FNR frequencies is shown in Fig. 2(c). The electromotive force spectrum exhibits two broad peaks around the frequency 200 and 350 MHz, corresponding to the ^{59}Co and ^{55}Mn FNR spectra. Although these peaks are broaden compared with the FNR spectrum especially in ^{59}Co FNR, which is attributed to the surface effect, this voltage signal implies that the FNR generates a spin current into the Pt layers.

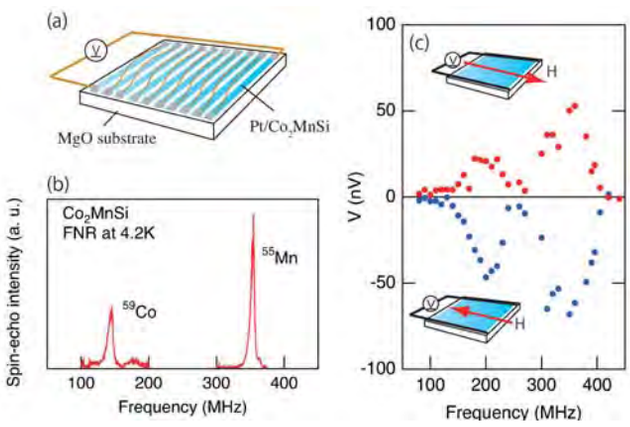

Fig. 2 (a) A schematic diagram of the sample set-up. (b) FNR spectra of ^{59}Co and ^{55}Mn. (c) The electromotive force between electrodes on the Pt layer arising from ^{59}Co and ^{55}Mn FNR.

Research Group for Reactions Involving Heavy Nuclei

Group Leader : Satoshi Chiba
Members : Katsuhisa Nishio, Shinichi Mitsuoka, Hroyuki Koura, Ichiro Nishinaka, Yutaka Utsuno, Hiroyuki Makii, Yasuo Wakabayashi, Yoshihiro Aritomo, Shuya Ota, Tatsuro Nagayama

The research objective of our group is to investigate heavy-ion induced reactions such as nucleon-transfer and fusion reactions. One subject is to develop experimental and theoretical methods to determine neutron-induced reaction cross sections with heavy-ion reactions. For nuclei with short half-lives, it is practically impossible to measure the cross sections in experiments using neutron source. The idea of the so-called surrogate reaction method is to populate the same compound nucleus as the neutron-capture reaction by nucleon-transfer reactions using available target nucleus and to measure the decay probabilities for fission and gamma-ray emission to derive fission and capture cross sections. In addition, nuclear fission and nuclear structure of exotic nuclei and reaction mechanism to produce exotic nuclei are in our scope.

Neutron-induced fission cross section of short-lived nucleus ^{239}U determined by surrogate reaction method

Neutron-induced fission cross sections for ^{239}U (half-life 23.5 min) were determined using the surrogate reaction technique. The compound nucleus $^{240}U^{*}$ was populated by the transfer-reaction ^{238}U(^{18}O,^{16}O)$^{240}U^{*}$, and the fission probability of $^{240}U^{*}$ was determined experimentally. The fission cross sections were obtained by refering the know fission cross sections of ^{235}U(n,f) and measuring the fission probability of $^{236}U^{*}$ populated by the reaction ^{235}U(^{18}O,^{17}O)$^{236}U^{*}$. The experiment was carried out at the JAEA tandem accelerator facility. A thin uranium target layer was bombarded by oxygen beams with 162 MeV. The transfer channel was identified by detecting the projectile-like nucleus using silicon ΔE-E detectors. Fission events were identifeid by detecting fission fragments with multi-wire proportional counters. The results are shown in Fig. 1.

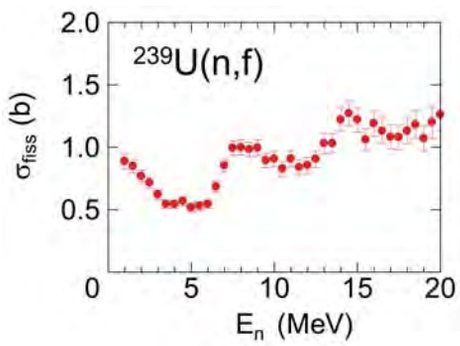

Fig. 1 Neutron-induced fission cross sections (in barn) for ^{239}U(n,f) plotted as a function of neutron energy (preliminary). The step structure associated with the first chance fission is seen at E_n = 7 MeV.

Reaction dynamics in collisions between heavy nuclei in the framework of fluctuation-dissipation model

Exotic nuclei far from stable isotopes are produced by collisions between heavy nuclei. An example is super-heavy nuclei (SHN), which can be produced by fusion-evaporation reactions. Understanding the fusion process is essential to predict the cross section for SHN and to make an experimental strategy. We have developed a model to calculate the evolution of nuclear shape from the initial impact between a projectile nucleus and an actinide target nucleus in the framework of fluctuation-dissipation model [1]. The actinide nucleus is prolately deformed, so that we have effectively taken into account the orientation effects on the reaction. Figure 1 shows the time evolutions of nuclear shape for systems produced by the ^{30}Si + ^{238}U and ^{36}S + ^{238}U reactions. Fusion is defined as the case that the nuclear shape attains the one of ground state of SHN (compound nucleus). The calculation shows the difference between fusion-fission and quasifission in the mass asymmetry of fission fragments and in the time scale for fission. The fusion probability is obtained from the fusion-fission yield relative to the total fission yield. The probability agreed with those determined by the evaporation residue cross sections [2,3]. The same model successfully described the nucleon-transfer induced fission [4].

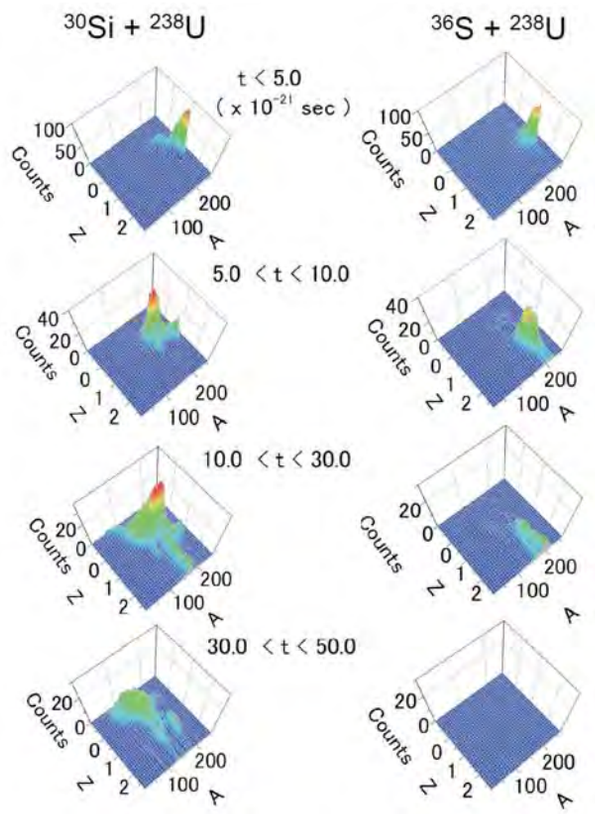

Fig. 2 Time evolutions of the probability distribution on the nuclear shape projected on on the mass asymmetry (mass unit) and charge-center distance for the systems produced in the reactions of ^{30}Si + ^{238}U (left) and ^{36}S + ^{238}U (right). Quasifission finishes at the time less than 30×10^{-21} s, whereas fusion-fission appears later than 30×10^{-21} s.

References

[1] Y. Aritomo *et al.*, Phy. Rev. C **85**, 044614 (2012).
[2] K. Nishio *et al.*, Phys. Rev. C **82**, 024611 (2010).
[3] K. Nishio *et al.*, Phys. Rev. C **82**, 044604 (2010).
[4] Y. Aritomo *et al.*, Phys. Rev. C **84**, 024602 (2011).

Research Group for Superheavy Elements

Group Leader : Matthias Schädel
Members : Kazuaki Tsukada, Masato Asai, Tetsuya Sato, Atsushi Toyoshima, Zijie Li, Nozomi Sato, Kazuhiro Ooe, Yuichiro Nagame

The research objectives of this group are to understand chemical and nuclear properties of superheavy elements (SHEs) placed at the uppermost end of the Periodic Table and on the heaviest frontier of the nuclear chart. To clarify the chemical properties of SHEs, we investigate valence electronic structures of SHEs through experimental determinations of ionization potentials, redox potentials, and compound formations of SHEs. To elucidate the limits of stability of the heaviest nuclei, we investigate the shell structure of superheavy nuclei through experimental assignments of proton and neutron single-particle orbitals and through the evolution of nuclear deformation at the highest proton and neutron numbers.

Element 104, rutherfordium (Rf) is the first transactinoid element. From the simple extension of the Periodic Table of the Elements, Rf should belong to the group 4 transition metals. Although chemical properties of Rf are expected to be similar to those of lighter homologues Zr and Hf, some differences are found in HCl and HF solutions [1,2], which provides valuable information on the valence electronic structure of Rf.

Fluorido complex formation of Rf in HF/HNO_3 mixed solution [3]

In the present work, we have investigated the cation-exchange behavior of ^{261}Rf ($T_{1/2}$ = 78 s) produced in the ^{248}Cm(^{18}O, 5*n*) reaction on a "one-atom-at-a-time" scale using an automated ion-exchange separation apparatus coupled with the detection system for alpha-spectroscopy (AIDA), together with its lighter group-4 homologs Zr and Hf, and the tetravalent pseudo-homolog Th in HF/HNO_3 mixed solution. The results demonstrate that distribution coefficients (K_d) of Rf in HF/0.10 M HNO_3 decrease with increasing concentration of the fluoride ion [F^-] (Fig. 1). This resembles the behavior of the homologs, indicating the consecutive formation of fluorido complexes of Rf. We also measured the K_d values of Rf and the homologs as a function of the hydrogen ion concentration [H^+] in the range of [F^-] = 5.29 × 10^{-7}–3.17 × 10^{-6} M. The logK_d values decrease linearly with an increase of log[H^+] with slopes between −2.1 and −2.5. This indicates that these elements are likely to form the same chemical compounds: mixture of $[MF]^{3+}$ and $[MF_2]^{2+}$ (M = Rf, Zr, Hf, and Th) in the studied solution. It is also ascertained that the fluorido complex formation of Rf is significantly weaker than that of Zr and Hf, but it is stronger than that of Th.

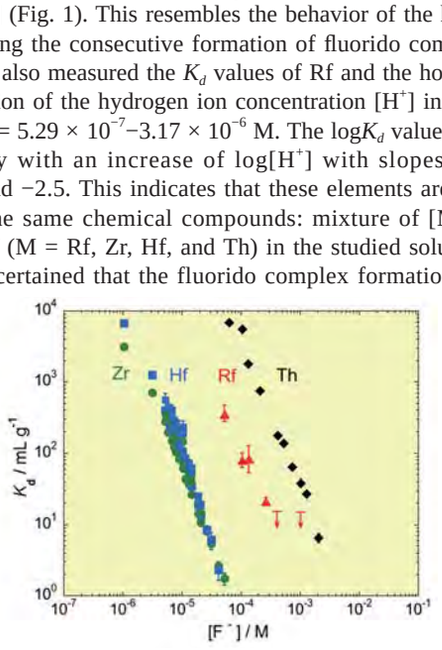

Fig. 1 Distribution coefficients, K_d, of Rf, Zr, Hf, and Th between a cation-exchange resin CK08Y and 0.10 M HNO_3 plotted as a function of [F^-].

Sulfate complex formation of Rf in H_2SO_4/HNO_3 mixed solution [4]

The cation-exchange behavior of Rf was studied in 0.15−0.69 M H_2SO_4/HNO_3 mixed solutions ([H^+] = 1.0 M) using AIDA. It was found that adsorption probabilities (%ads) of ^{261}Rf on cation-exchange resin decrease with an increase of [HSO_4^-], showing a successive formation of Rf sulfate complexes. Rutherfordium exhibits a weaker complex formation tendency compared to the lighter homologues Zr and Hf. This is in good agreement with theoretical predictions including relativistic effects [5]. It was shown that the lower stability of the Rf complexes is due to the smaller ionic contribution to the chemical bond, which is caused by the relativistic stabilization of the 7s orbital, as well as the destabilization and spin-orbit splitting of the 6*d* orbitals. It is also in agreement with its larger ionic radius (76 pm) [6] in comparison with those of Zr (71 pm) and Hf (72 pm) [7]. We like to compare this results with our previous report for the complex formation with fluoride ions [2,3]. The trend of the fluoride complex formation in the group-4 elements is Zr ≈ Hf > Rf > Th, being also in agreement with theoretical predictions [8]. The smaller ionic contribution to the metal–fluorine bonding was also responsible for the weaker fluoride complexation of Rf in comparison with that of Zr and Hf [8].

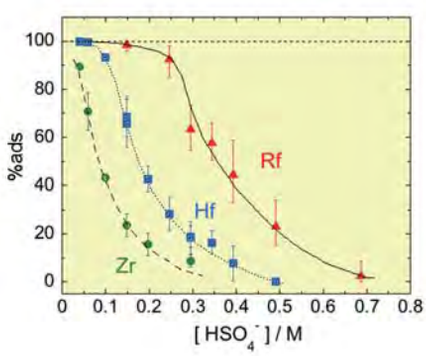

Fig. 2 Variations of adsorption probabilities, %ads, of Rf, Zr, and Hf on a cation-exchange resin CA08Y as a function of [HSO_4^-] in the H_2SO_4/HNO_3 mixed solutions ([H^+] = 1.0 M).

References

[1] H. Haba *et al*., J. Nucl. Radiochem. Sci. **3**, 143 (2002).
[2] A. Toyoshima *et al*., Radiochim. Acta **96**, 125 (2008).
[3] Y. Ishii *et al*., Bull. Chem. Soc. Jpn. **84**, 903 (2011).
[4] Z. J. Li *et al*., Radiochim. Acta **100**, 157 (2012).
[5] V. Pershina *et al*., Radiochim. Acta **94**, 407 (2006).
[6] V. Pershina, "Theoretical chemistry of the heaviest elements", in *The Chemistry of Superheavy Elements* (M. Schädel, ed.), Kluwer Academic Publisher, Dordrecht (2003).
[7] R. Shannon, Acta Cryst. A **32**, 751 (1976).
[8] V. Pershina *et al*., Radiochim. Acta **90**, 869 (2002).

Research Group for Actinide Materials Science

Group Leader : Zachary Fisk
Members : Yoshinori Haga, Etsuji Yamamoto, Naoyuki Tateiwa, Tatsuma D. Matsuda, Yuji Matsumoto, Akio Nakamura

5*f* electrons in actinide compounds play essential roles in various phase transitions in actinide compounds. The electronic states can be modified by the chemical or physical environment around these electrons. It is therefore interesting to investigate new materials under various conditions such as pressure, magnetic field or low temperature to find new phenomena. The purification of a known compound also provides new insight particularly for phenomena occurring at low temperatures, where impurity disorder can deeply disturb and hence hide the intrinsic behavior.

Superconductivity and hidden-order in URu_2Si_2 investigated with high-quality sample and high-pressure technique

One of the problems in condensed-matter physics is the superconductivity occurring in strongly correlated electron systems where an unconventional type of pairing interaction is required. A uranium intermetallic compound URu_2Si_2 shows 'heavy fermion' superconductivity where the effective mass of conduction electrons is much larger than that of conventional metals. It is known that this superconductivity coexists with a so-called 'hidden-order' state where some of the electronic degrees of freedom order. Although extensive studies have been carried out for more than 25 years, the order parameter characterizing the 'hidden-order' is not established. We investigated the peculiar properties of the superconductivity and hidden-order phase by analyzing the impurity effects and extracted intrinsic behavior which is only seen in high-quality single crystals, as shown in Fig. 1 [1]. The study is further extended to high-pressure phase where both the 'hidden-order' and superconducting transition temperature vary and are finally replaced by an antiferromagnetic order. From this study, an unusual electron scattering in the 'hidden-order' state relevant to superconductivity was found [2]. See 'Research Highlights' for details.

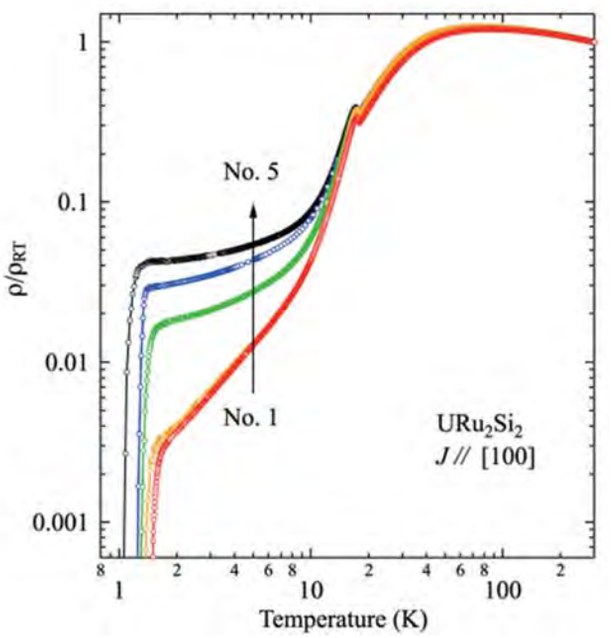

Fig. 1 Temperature dependence of electrical resistivity measured of URu_2Si_2 single crystals with different residual resistivities. The low temperature behavior as well as the superconducting transition temperature strongly depend on the crystal quality.

New neptunium-gallium intermetallic phases

Successive crystal transformations as a function of temperature or pressure are one of the prominent properties observed in actinide elemental metals. In contrast to elemental metals, however, such structural transitions are not likely to occur in compounds because they are composed of more than two kinds of atoms and such structural transitions usually accompany changes in the arrangement of the different atomic species. It is therefore worth investigating the metallic phase diagram at lower temperatures to look for possible occurrences of low-temperature phases. Most previous studies on actinide binary phases have been performed using arc-melted samples where the high-temperature melt typically around 1,500 ˚C is quenched to low temperature. We investigated Np-Ga phases using Gallium flux technique where the crystal growth takes place below 1,000 ˚C. The previous study reports $NpGa_3$ with cubic $AuCu_3$-type structure. We found trigonal phase of $NpGa_3$ instead of cubic phase and a new compound Np_3Ga_{11} [3]. As shown in Fig. 2, the structure of both compounds conserves a local atomic arrangement similar to that in the cubic $AuCu_3$-type structure.

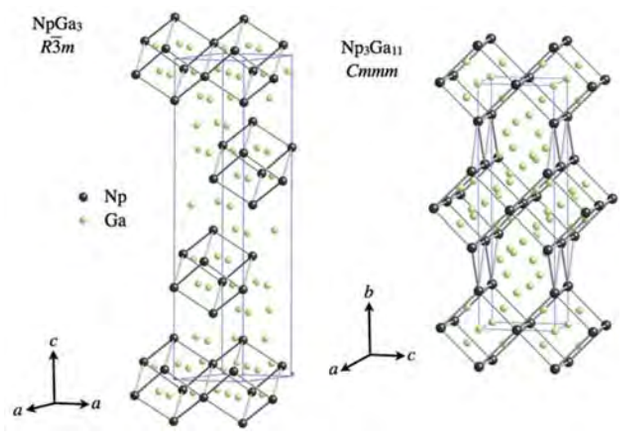

Fig. 2 Crystal structure of trigonal $NpGa_3$ and Np_3Ga_{11}.

References

[1] T. D. Matsuda *et al*., J. Phys. Soc. Jpn. **80**, 114710 (2011).
[2] N. Tateiwa *et al*., Phys. Rev. B **85**, 054516 (2012).
[3] Y. Haga *et al*., J. Phys. Soc. Jpn. **80**, SA109 (2011).

Research Group for Condensed Matter Physics of Heavy Element Systems

Group Leader : Shinsaku Kambe
Members : Wataru Higemoto, Yo Tokunaga, Hironori Sakai, Takashi U Ito, Kazuhiko Ninomiya

In heavy element (*f*-electron) systems, valence fluctuations, the Kondo effect, and the RKKY interaction compete with one another. Because of this, exotic behaviors such as quantum critical points, heavy fermions, non-Fermi liquids, anisotropic superconductivity and multipolar ordering appear when such competition is strong. Recently, it has become clear that these exotic behaviors for 5*f*-electron systems are different from those for 4*f*-electrons. This is because electrons with different spin and orbital character can coexist in 5*f* actinide systems, in contrast to the case of 4*f* electrons. By means of microscopic spectroscopy: NMR and μSR, our research group tries to clarify these exotic behaviors due to the "many-fold" character of both 4f and 5*f* compounds, including transuranium.

Non-collinear antiferromagnetic ordering and new type of multipolar frustration in $TbCoGa_5$

$HoCoGa_5$ type structure (115) compounds are particularly interesting since many fascinating phenomena are observed *i.e.* unconventional superconductivity near a magnetic quantum critical point (as shown in research highlight for $CeCoIn_5$), and phase transition related with multipolar ordering. In this context, it is quite important to understand magnetic interactions between *f*-electrons in the 115 systems. A 115 type compound $TbCoGa_5$ shows successive two antiferromagnetic transitions. From neutron diffraction measurements, there are two ordered states AF-I (high T phase below T_{N1}=36 K) and AF-II (low T phase below T_{N2}=5.4 K). Tb moments order in a stripe fashion along the *c*-axis in the AF-I phase, and an ordering in the ab-plane is finally established in the AF-II phase. Unfortunately, the neutron measurements could not distinguish collinear from non-collinear structure of the AF-II phase. If non-collinear structure is the case, it is particularly interesting since such behaviour suggests a magnetic frustration in the ab-plane.

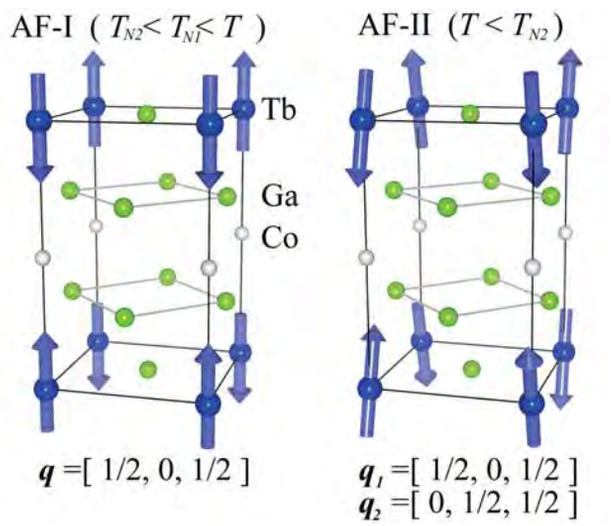

Fig. 1 Antiferromagneically ordered structures in $TbCoGa_5$. Collinear AF I at high temperatures $T_{N2}<T<T_{N1}$ (left) and non-Collinear AF II at low temperatures $T<T_{N2}$ (right). $\boldsymbol{q}$ is ordering wave vector.

Based on the Ga-NMR in $TbCoGa_5$, the AF-II has been actually identified as non-collinear phase for the first time (Fig. 1) [1]. Generally, non-collinear structure can appear to reduce frustration, whereas there is no geometrical frustration in $TbCoGa_5$, indicating that there may be a new mechanism of frustration. Now a possible mechanism *i.e.* frustration between dipolar and quadrupolar interactions is investigated.

Coexistence of superconductivity and multipolar ordering in $PrIr_2Zn_{20}$

$PrIr_2Zn_{20}$ belongs to caged compounds RT_2X_{20} having the cubic $CeCr_2Al_{20}$-type structure where R atoms are encapsulated in cages formed by 16 zinc atoms. In a RT_2X_{20} system, a multipole phase transition is expected to occur owing to the highly degenerate ground state. Among these systems, $PrIr_2Zn_{20}$ is particularly interesting since ac-magnetic susceptibility measurements revealed superconductivity below 0.05 K. Furthermore, recent low-temperature specific heat measurements reveal another phase transition below 0.11 K, although the origin of transition has not been identified.

To elucidate magnetic and superconducting properties, we performed muon spin rotation and relaxation measurements (μSR) in $PrIr_2Zn_{20}$ at very low temperatures [2]. As shown in Fig. 2, temperature independent μSR spectra were observed below 1 K, indicating that a phase transition at 0.11 K is of a non-magnetic origin, most probably pure quadrupole ordering. In the superconducting phase, no sign of unconventional superconductivity, such as superconductivity with broken time-reversal symmetry, was seen below T_c=0.05 K. The present measurement indicates that a coexistence of superconductivity and quadrupolar ordering may be realized in $PrIr_2Zn_{20}$. Now relation between the superconductivity and quadrupolar fluctuations is investigated.

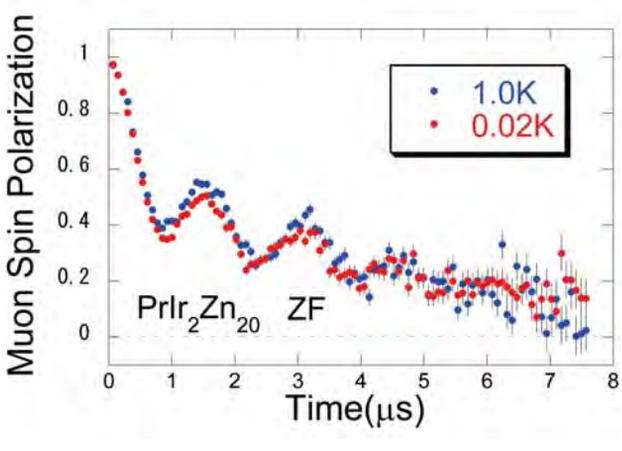

Fig. 2 Zero field (ZF) μSR spectra in $PrIr_2Zn_{20}$ at 1.0 K and 0.02 K.

References

[1] Y. Tokunaga *et al.*, Phys. Rev. B **84**, 214403 (2011).
[2] W. Higemoto *et al.*, to appear in Phys. Rev. B.

Research Group for Hadron Physics

Group Leader : Ken-ichi Imai
Members : Toshiki Maruyama, Hiroyuki Sako, Susumu Sato, Shoichi Hasegawa, Kotaro Shirotori, Ryuta Kiuchi, Kiyoshi Tanida, Hitoshi Sugimura, Yudai Ichikawa, Minoru Okamoto

The research objectives of Hadron Physics Research Group are: (i) empirical study of structure of nuclei and hadrons with strangeness, with use of high intensity $K(\pi)$-beams at J-PARC, and (ii) theoretical study of nuclear matter, hadrons with strangeness, and high density matter realized in neutron stars.

In JFY 2011, we have (1) searched for pentaquarks Θ^+ at J-PARC (E19) and established new upper limits, (2) proposed an experiment for H-dibaryon at J-PARC (P42), and (3) developed and installed vertex pixel detector for charm/bottom tagging at BNL−RHIC PHENIX experiment to study high energy heavy ion collisions. Also we have studied (4) high density matters in theoretical simulations, in which phase transitions of baryon density distribution has been found at the surface of the neutron star.

Experimental search for pentaquarks Θ^+

The Θ^+ baryon has been searched for via the $\pi^- p \rightarrow K^- X$ reaction using a 1.92 GeV/c π^- beam at the J-PARC−K1.8 beam line. The K1.8 beam line spectrometer and the SKS spectrometer shown in Fig. 1, both of which have an excellent momentum resolution, were used. In the missing mass spectrum, no prominent peak has been observed (Fig. 2) in the Θ^+ mass region [1]. The preliminary upper limit of the differential cross section averaged over the scattering angle from 2 to 15 degrees at the laboratory frame was less than 0.3 μb/sr at the 90% confidence level in the missing mass region of 1.51–1.55 GeV/c^2.

Study of the exotic state with strangeness; H-dibaryon

One of the exotic hadronic states, composed of 6 quarks, is H-dibaryon ("uuddss" quark state). In order to observe such a state, a large acceptance tracking spectrometer is indispensable. We have been doing R&D for a Time Projection Chamber (TPC), and Silicon Strip Detectors (SSDs) with Seoul National University and Scintillating Fiber trackers (SciFi) with Tohoku University as high-rate pion and kaon beam line trackers. A beam test has been performed at RCNP in Nov. 2011, and good performance (at 10^6 of incident beam rate) of these detectors was obtained (e.g., in TPC, a few 100s micrometer resolution was achieved). Design of the spectrometer is progressing in collaborating with Pusan National University.

Study of heavier flavour (charm/bottom) in heavy ion collision

We have developed and installed a vertex pixel detector in collaboration at BNL-RHIC PHENIX experiment, to extrapolate the signal from particle with charmed and/or bottom flavours. In 2011 and 2012, we have accumulated collision data of Au + Au and Cu + Au.

Numerical study of inhomogeneous structures in nuclear matter

We have numerically explored the pasta structures [3] and properties of low-density nuclear matter without any assumption on the geometry. We observed conventional pasta structures, while a mixture of the pasta structures appeared as a metastable state at some transient densities. Proton density distributions of the ground states of symmetric matter are shown in Fig. 3. Typical pasta structures were observed: (a) Spherical droplets at baryon density of 0.01 fm^{-3}. (b) Cylindrical rods with a honeycomb crystalline structure at 0.024 fm^{-3}. (c) Slabs at 0.05 fm^{-3}. (d) Cylindrical tubes with a honeycomb crystalline structure at 0.08 fm^{-3}. (e) Spherical bubbles at 0.09 fm^{-3}.

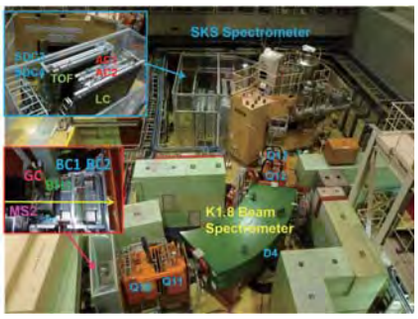

Fig. 1 K1.8 beam line spectrometer and the SKS spectrometer at J-PARC.

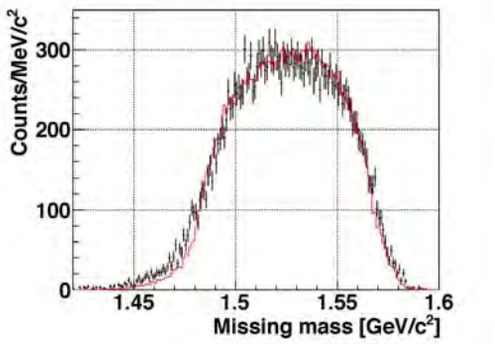

Fig. 2 Missing mass spectrum distribution via $\pi^- p \rightarrow K^- X$ reaction using a 1.92 GeV/c π^- beam. The red histogram shows corresponding background.

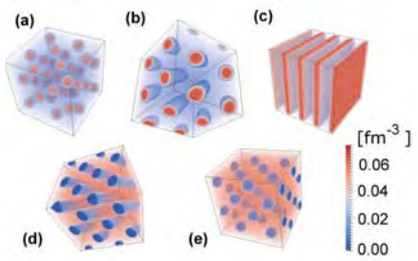

Fig. 3 Proton density distributions of the ground states of symmetric nuclear matter. For details, see the text.

References

[1] K. Shirotori *et al.*, The Fifth Asia-Pacific Conference on Few-Body Problems in Physics, **APBF2011** (2011).
[2] Program Advisory Committee (PAC) for Nuclear and Particle Physics Experiments at the J-PARC 50 GeV Proton Synchrotron: http://j-parc.jp/researcher/Hadron/en/PAC_for_NuclPart_e.html, **J-PARC PAC** (2011).
[3] T. Maruyama and T. Tatsumi, J. Phys. Conf. Ser. **312**, 042015 (2011).

Research Group for Bioactinide

Group Leader : Toshihiko Ohnuki
Members : Naofumi Kozai, Fuminori Sakamoto, Shinya Yamasaki, Mingyu Jiang, Shousuke Igarashi

The research objectives of Bioactinides Chemistry Research group are elucidate chemical states change of actinides and lanthanides including nano-particles formation in the biological reaction environments. In the year of 2011, chemical states change of lanthanides by the transfer of phosphorous ions and electron from the cells to lanthanides has been studied.

Formation of phosphate nano-particles in the biological reaction environments

Phosphate minerals containing heavy elements of lanthanides and U are known to be hardly soluble in the aqueous solution in the environments. Phosphorous is an essential element of microorganisms. The microorganisms store P in their cells. We have found that yeast, *Saccharomyces cerevisiae* releases P in solution containing Ce(III), followed by the formation of cerium phosphate mineral of monazite [1]. However, not only mechanism of the formation of REE phosphate mineral, but role of microorganisms for the formation have not been elucidated.

When the yeast cells are exposed to the solution containing 1.44×10^{-4} mol/L Yb(III) (heavy REE) for 2-120 h, and two months at 25 ± 1 °C at an initial pH of 3, 4, or 5, Yb concentrations in solutions decreased as a function of exposure time [2]. Field-emission scanning electron microscopy equipped with energy-dispersive X-ray spectroscopy (FESEM), and transmission electron microscopy (TEM) analyses revealed that nano-sized blocky Yb phosphate with an amorphous phase formed on the yeast cells surfaces in the solutions with Yb. These nano-sized precipitates that formed on the cell surfaces remained stable without changing their size even after two months of exposure at 25 ± 1 °C around neutral pHs.

The synchrotron-based extended X-ray absorption fine structure (EXAFS) analysis revealed that the chemical state of the accumulated Yb on the cell surfaces changed from the adsorption on both phosphate and carboxyl sites at 30 min to Yb phosphate precipitates at 5 days, indicating the Yb-phosphate precipitation as a major post-adsorption process. In addition, the precipitation of Yb phosphate occurred on cell surfaces during 7 days of exposure in Yb-free solution after 2 h of exposure (short-term Yb adsorption) in Yb solution. These results suggest the transformation of the adsorbed Yb to Yb phosphate precipitates on cell surfaces, even though no P was added to the exposure solution. In an abiotic system, the EXAFS data showed that the speciation of sorbed Yb on the reference materials, carboxymethyl cellulose and Ln resin, did not change even when the Yb was exposed to P solution, without forming Yb phosphate species. This result strongly suggests that the cell surface of the yeast plays an important role in the Yb-phosphate precipitation process, not only as a carrier of the functional groups but also as a substrate inducing the nucleation of phosphate nanoparticles.

These results indicate that light and heavy REEs behave different manner at the biological reaction environments. This fact stimulates us to investigate the behaviour of series of REEs at the biological reaction environment. We have a plan to study on the behavior of series of REEs by yeast.

Chemical states change of REEs - desferrioxamine B complexes by *Pseudomonas fluorescens* and γ-Al_2O_3

Biological materials possess functional groups able to complex with metal cations. Siderophores are microbial chelating agents produced to solubilize Fe(III). Desferrioxamine (DFO) B is a trihydroxamate siderophore ubiquitously found in the environment and its interaction with various metal cations has been studied. We found that at pH 7 negative adsorption anomaly of Ce on *P. fluorescens* cells and γ-Al_2O_3 compared to the neighbouring REEs(III), La(III) and Pr(III); this was because the oxidization of Ce(III) to Ce(IV) during complexiation with DFO and the higher stability of the Ce(IV)-DFO complex than that of the Ce(III)-DFO complex and the La(III)- and Pr(III)-DFO complexes [3].

In this study, we have studied the interactions of REEs (La, Ce, Pr, Nd, Sm, Eu, Gd, Tb, Dy, Ho, Er) - DFO complexes with *P. fluorescens* cells and with γ-Al_2O_3, at pH 4 – 9. The higher percent adsorption of REEs was obtained at lower pHs on *P. fluorescens* cells and at higher pHs on γ-Al_2O_3. Degree of negative anomaly of Ce compared to its neighbouring REEs, La(III) and Pr(III) decreased with increasing pH. XAFS analysis showed that Ce exists as the Ce(IV)-DFO complex in higher pH than 6. Thus, the pH dependence of Ce anomaly is predominantly dependent on the stability of Ce(IV)-DFO complex.

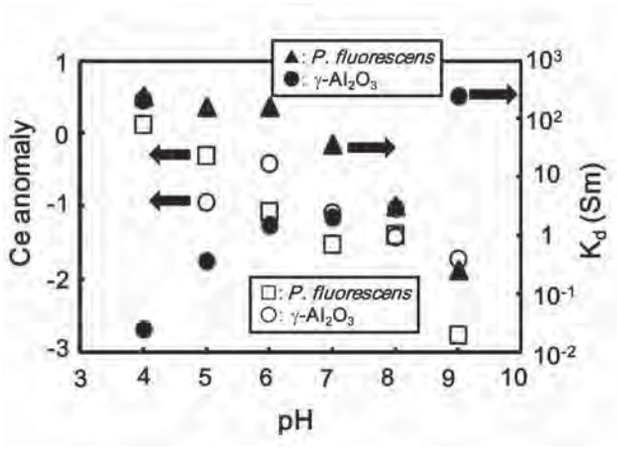

Fig. 1 Degrees of Ce anomaly and K_d(Sm) on *P. fluorescens* cells and γ-Al_2O_3 as a function of pH.The degree of Ce anomaly for the K_d(REE) patterns was expressed by: $DA = \log K_d(Ce) - [\log K_d(La) + \log K_d(Pr)]/2$.

References

[1] M. Jiang *et al*., Chemical Geology, **277**, 61(2010).
[2] M. Jiang, Thesis Kyushu Univ. (2012).
[3] T. Ohnuki, T. Yoshida, Chemistry Letters, **41**, 98(2011) .

Research Group for Radiation and Biomolecular Sciences

Group Leader : Akinari Yokoya
Members : Kentaro Fujii, Miho Noguchi, Ayumi Urushibara, Toshitaka Oka, Yuki Sugaya, Iyo Shiraishi, Takuya Shiina

The research objective of the research group is to fully characterize molecular processes by which ionizing radiation alters the chemical structure of DNA in cells. Two approaches were proposed to address the main objective: 1) Obtain experimental evidence of repairability of artificial clustered DNA damage *in vitro*. 2) Determine the yields of DNA lesions in a simple model DNA molecule, in terms of LET (Linear Energy Transfer) as an index of charged particle-radiation.

***In vitro* study of repairability of 8-oxoG/single strand break-containing clusters depends on their relative positions**

The biological consequences of clusters DNA damage site containing a single strand break (SSB) and nucleobase lesion(s) remain largely unknown. We examined the repairbility of two- and three-lesion clustered damage sites containing a 1-nucleotide gap (GAP) and 8-oxo-7,8-dihydroguanine(s) (8-oxoG(s)) by a base excision repair enzyme, Fpg, *in vitro* [1]. Fpg specifically excises purine base lesions such as 8-oxoG residues from DNA backbone via its AP lyase activity, and subsequently cleaves the DNA. The processing of the tandem cluster by Fpg leads to the generation of an additional band with a slightly larger size (18 mer OH termini) than that observed after excision of a single 8-oxoG (Fig. 1).

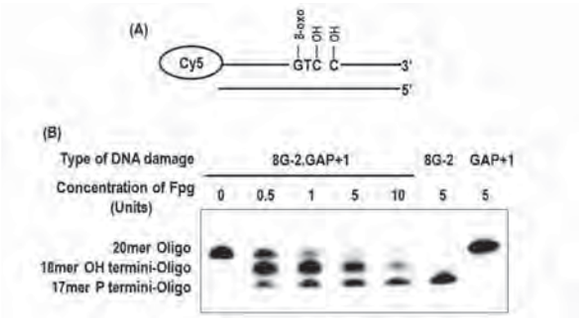

Fig. 1 Gel image of the excision of an 8-oxoG by Fpg placed in tandem with a GAP. (A) The shematic diagram of a Cy5-labeled double stranded oligonucleotide containing a GAP and an 8-oxoG tamdem clsuter. (B) 5' Cy5-labeled tandem cluster (8G-2, GAP+1) was incubated with increasing amounts (0-10 units) of Fpg. The configuration of the tandem cluster is indicated above the gel. 5' Cy5-labeled duplex oligonucleotides containing a single 8-oxoG (8G-2) incubated with Fpg and a single GAP (GAP+1) are shown for comparison.

The activity of the enzyme causes successive β- and δ-elimination reactions and generates a 1-nt gap. We treated the cluster with 0.1M NaOH, as an alkaline treatment is known to convert the β-elimination product to δ-elimination product at the 3' end. The result that the additional band disappeared after the alkaline treatment indicates that the band corresponds to a fragment generated by β-elimination. Further, to look at the effect of an additional 8-oxoG on the opposite strand for the excision of the 8-oxoG placed with a GAP in tandem, a three-lesion cluster (two 8-oxoGs and one GAP) was treated with Fpg. The 8-oxoG in tandem with a GAP in the three-lesion cluster is excised in a fashion similar to the excision of the 8-oxoG with a GAP in the tandem two-lesion cluster, forming two bands. This indicates that the additional 8-oxoG on the complementary strand does not inhibit the action of Fpg at the 8-oxoG placed with a GAP in tandem.

LET dependence of the yield of DNA damage induced in fully hydrated DNA films by ion particle-irradiation

In order to clarify the characteristics of DNA damage induced by high LET charged particle-radiation, the yield of DNA damage induced in closed-circular plasmid DNA (pUC18) were measured after exposing to various kinds of radiation (He, Ne and C ions; 2 to 900 keV/μm) using the JAEA-TIARA and NIRS-HIMAC facilities [2]. Hydrated DNA samples were used together with base excision repair enzymes, Fpg (see above) and EndoIII, which mainly excises pyrimidine base lesions, to detect the lesions as enzyme sensitive sites (ESSs). The results show that 1) the yields of ESS decrease drastically with increasing LET and very few ESSs are induced >100 keV/μm, althoguh the yield of SSB does not depend significantly on LET of the ions (Fig. 2), 2) the yield of duble strand breaks (DSBs) increases with increasing LET, however, 3) those of clustered damage sites visualized as additional DSBs by enzymatic treatment decrease with increasing LET, and 4) C and Ne ions induce less nucleobase lesions than He ions for comparable LET values. These results indicate that the yields of clusters containing nucleobase lesions, which are less readily processed by the base excision repair enzymes, depend not only on LET but also on the ion particle used.

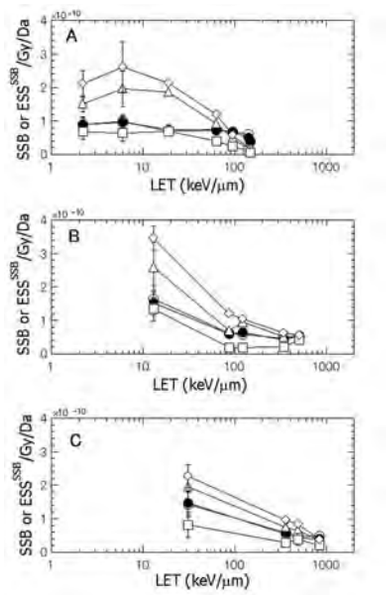

Fig. 2 Dependence of the yield of SSB or n(ESS or SSB) on LET for fully hydrated DNA irradiated with $^{4}He^{2+}$ ions (A), $^{12}C^{5+,6+}$ (B) and $^{20}Ne^{8+,10+}$ (C) at 5.6 °C (○), or following post-irradiation incubation for 30 min at 37 °C in the absence (●) or presence of either Nth (△), Fpg (□), or both Nth and Fpg (◇). The yields of isolated nucleobase lesions visualized by the enzymatic treatment decrease drastically with increasing LET.

References

[1] M. Noguchi *et al*., Mutat. Res. **732**, 34 (2012).
[2] T. Ushigome *et al*., Radiat. Res. **177**, 614 (2012).

Research Group for Spin-Polarized Positron Beam

Group Leader : Atsuo Kawasuso
Members : Masaki Maekawa, Yuki Fukaya, Izumi Mochizuki, Atsushi Yabuuchi

The research objectives of Spin-Polarized Positron Beam Group are to promote spintronics material study using a highly spin-polarized positron beam. Using a positron source (^{68}Ge-^{68}Ga) produced through a nuclear reaction, we develop a spin-polarized positron beam. After establishing the foundation of spin-polarized positron annihilation spectroscopy (SP-PAS) from both experimental and theoretical viewpoints, using SP-PAS method, we study spintronics materials and novel spin phenomena.

Construction of spin-polarized positron beam line using a ^{68}Ge-^{68}Ga source

To conduct spintronics study extensively, we need to have a spin-polarized positron beam. The performance required for the spin-polarized positron beam is as follows: (i) Higher spin polarization, (ii) Energy tunability from several eV to tenth keV, (iii) Polarization switchability between longitudinal and transverse directions. To fulfill the above requirements, we produced a ^{68}Ge-^{68}Ga source which emits highly spin-polarized positrons as compared to the conventional ^{22}Na source and constructed an electrostatic beam line as shown in Fig.1 [1]. The ^{68}Ge-^{68}Ga source was produced through a proton nuclear reaction ^{69}Ga(p, 2n)^{68}Ge. For an efficient production of ^{68}Ge-^{68}Ga, we first used an isotope-separated ^{69}Ga metal as a target material. However, melted Ga reacted with the capsule materials and eventually destroyed the capsule itself. We therefore replaced the ^{69}Ga metal with a GaN crystal and have been repeating irradiation experiment more than fifteen times since April/2010. The current activity of the ^{68}Ge-^{68}Ga source gets to approximately 300 MBq. Consequently, we succeeded to generate a spin-polarized positron beam with a flux of 5×10^3 e^+/sec and a polarization of more than 35 %. We also confirm that, by changing the energy selector between magnetic and electrostatic deflectors, the polarization direction can be changed between longitudinal and transverse. Using this spin-polarized positron beam, we could observe the magnetic-field-reversal asymmetry of the Doppler broadening of annihilation radiation spectra.

Spin Hall effect on a Pt(001) surface observed by spin-polarized positron annihilation

The spin Hall effect (SHE) is a phenomenon of electron spin flow, which occurs near non-magnetic conducting material surfaces under a direct current. The origin of SHE is thought to be the spin-orbit interaction between conduction electrons and nuclei. Conduction electrons with spins perpendicular to the charge current will be bent to the transverse directions for both the current and spin directions. Consequently, in-plane polarized electron spins appear near each surface surrounding the current axis. Recently, markedly large SHEs were reported in some metals, such as Pt and Au. Furthermore, direction of spin polarization is found to be different for different metal kinds. Experimental detection of metal SHE is normally done by using magnetotransport or ferromagnetic resonance measurements. These methods hardly determine polarization of electron spins appeared on metal surfaces due to SHE. In using a spin-polarized positron beam, we attempted to detect polarized electrons near the Pt(001) surface [2]. We found that the intensity of three-photon annihilation of spin-triplet positronium changes upon current reversal (Fig. 2) and the asymmetry in the intensity depends on angle between positron polarization and current directions as anticipated for SHE of Pt. The spin polarization of surface electrons near the Fermi level was evaluated to be more than 0.01 which is four orders of magnitude greater than that expected from a conventional spin diffusion theory. To explain the above experimental fact, some special surface effects such as the Rashba effect and surface ferromagnetism should be considered.

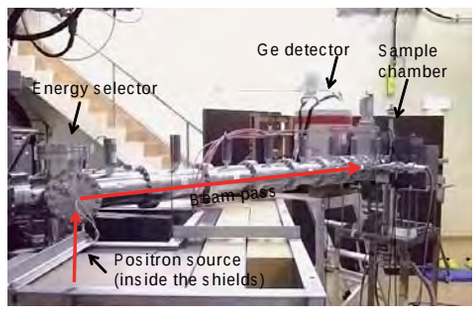

Fig. 1 Picture of newly developed spin-polarized positron beam line. The source part (surrounded by lead and concrete blocks) is directly connected to the proton irradiation chamber. The source strength is increased by repeating irradiation annually. The positron beam is lifted up from the positron gun, bent 90° and transported horizontally to the sample chamber. At the sample chamber, annihilation gamma rays are measured by a high-purity Ge detector.

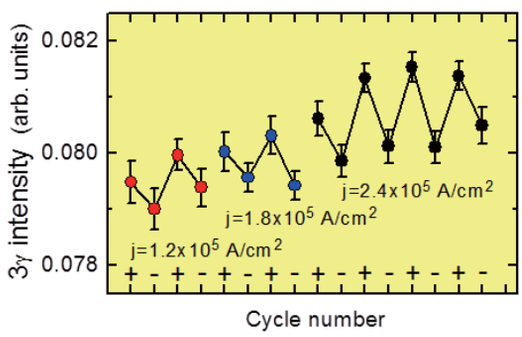

Fig. 2 Three-gamma annihilation intensity measured upon successive current reversal observed for the Pt(001) surface. (+) and (-) denote the direction of current applied for the sample. Current and positron spin polarization directions are perpendicular to each other. The oscillating behaviour of the three-gamma annihilation intensity upon current reversal means that spin-polarization of surface electrons is changed between parallel and anti-parallel with respect to the positron spin-polarization upon current reversal.

References

[1] M. Maekawa *et al*., Nucl. Inst. Meth. Phys. Res. B, submitted.
[2] A. Kawasuso *et al*., Phys. Rev. Lett., to be published.

Publication List

Research Group for Condensed Matter Theory

Papers

1) Thermoelectric response in the incoherent transport region near Mott transition: the case study of $La_{1-x}Sr_xVO_3$, M. Uchida, K. Oishi, M. Matsuo, W. Koshibae, Y. Onose, M. Mori, J. Fujioka, S. Miyasaka, S. Maekawa, and Y. Tokura, *Phys. Rev. B* **83**, 1651271-1-1651271-5 (2011).
2) Equation-of-motion approach of spin-motive force, Y. Yamane, J. Ieda, J. Ohe, S. E. Barnes, and S. Maekawa, *J. Appl. Phys.* **109**, 07C735-1-07C735-3 (2011).
3) Spin current generation due to mechanical rotation in the presence of impurity scattering, M. Matsuo, J. Ieda, E. Saitoh, and S. Maekawa, *Appl. Phys. Lett.* **98**, 242501-1-242501-3 (2011).
4) Composite excitation of Josephson phase and spin waves in Josephson junctions with ferromagnetic insulator, S. Hikino, M. Mori, S. Takahashi, and S. Maekawa, *J. Phys. Soc. Jpn.* **80**, 074707-1-074707-8 (2011).
5) Giant enhancement of spin accumulation and long-distance spin manipulation in metallic lateral spin valves, Y. Fukuma, L. Wang, H. Idzuchi, S. Takahashi, S. Maekawa, and Y. Otani, *Nature Materials* **10**, 527-531 (2011).
6) Electrically tunable spin injector free from the impedance mismatch problem, K. Ando, S. Takahashi, J. Ieda, H. Kurebayashi, T. Trypiniotis, C. Barnes, S. Maekawa, and E. Saitoh, *Nature Materials* **10,** 655-659 (2011).
7) Long-range spin Seebeck effect and acoustic spin pumping, K. Uchida, H. Adachi, T. An, T. Ota, M. Toda, B. Hillebrands, S. Maekawa, and E. Saitoh, *Nature Materials* **10**, 737-741 (2011).
8) Spinmotive force due to intrinsic energy of ferromagnetic nanowires, Y. Yamane, J. Ieda, J. Ohe, S. E. Barnes, and S. Maekawa, *Appl. Phys. Express* **4**, 193003-1-093003-3 (2011).
9) Spin-dependent inertial force and spin current in accelerating systems, M. Matsuo, J. Ieda, E. Saitoh, and S. Maekawa, *Phys. Rev. B* **84**, 104410-1-104410-9 (2011).
10) Li(Zn,Mn)As as a new generation ferromagnet based on a I-II-V semiconductor, Z. Deng, C.Q. Jin, Q.Q. Liu, X.C. Wang, J.L. Zhu, S.M. Feng, L.C. Chen, R.C. Yu, C. Arguello, T. Goko, Fanlong Ning, Jinsong Zhang, Yayu Wang, A.A. Aczel, T. Munsie, T.J. Williams, G.M. Luke, T. Kakeshita, S. Uchida, W. Higemoto, T.U. Ito, Bo Gu, S. Maekawa, G.D. Morris, and Y.J. Uemura, *Nature Communications* **2**, 422 (2011).
11) Continuous Generation of Spinmotive Force in a Patterned Ferromagnetic Film, Y. Yamane, K. Sasage, T. An, K. Harii, J. Ohe, J. Ieda, S. E. Barnes, E. Saitoh, and S. Maekawa, *Phys. Rev. Lett.* **107**, 236602-1-236602-4 (2011).
12) Nonmonotonic temperature dependence of thermopower in strongly correlated electron systems, M. Matsuo, S. Okamoto, W. Koshibae, M. Mori, and S. Maekawa, *Phys. Rev. B* **84**, 153107-1-153107-4 (2011).
13) Inverse spin-Hall effect induced by spin pumping in metallic system, K. Ando, S. Takahashi, J. Ieda, Y. Kajiwara, H. Nakayama, T. Yoshino, K. Harii, Y. Fujikawa, M. Matsuo, S. Maekawa, and E. Saitoh, *J. Appl. Phys.* **109**, 103913-1-103913-11 (2011).
14) Gutzwiller method for an extended periodic Anderson model with the c–f Coulomb interaction, K. Kubo, *J. Phys. Soc. Jpn.* **80**, 114711-1-114711-8 (2011).
15) Mass enhancement in an intermediate-valent regime of heavy-Fermion systems, K. Kubo, *J. Phys. Soc. Jpn.* **80**, 063706-1-063706-4 (2011).
16) Multipole correlations of t2g-orbital Hubbard model with spin-orbit coupling, H. Onishi, *J. Phys. Soc. Jpn.* **80** *Suppl. A*, SA141-1-SA141-3 (2011).
17) Correlation effects on antiferromagnetism in Fe pnictides, K. Kubo and P. Thalmeier, *J. Phys. Soc. Jpn.* **80**, *Suppl. A*, SA121-1-SA121-3 (2011).
18) Quantum dynamics of a driven correlated system coupled to phonons, L. Vidmar, J. Bonča, T. Tohyama, and S. Maekawa, *Phys. Rev. Lett.* **107**, 246404-1-246404-5 (2011).
19) Polarization-analyzed resonant inelastic x-ray scattering of the orbital excitations in $KCuF_3$, K. Ishii, S. Ishihara, Y. Murakami, K. Ikeuchi, K. Kuzushita, T. Inami, K. Ohwada, M. Yoshida, I. Jarrige, N. Tatami, S. Niioka, D. Bizen, Y. Ando, J. Mizuki, S. Maekawa, and Y. Endoh, *Phys. Rev. B* **83,** 241101-1-241101-4 (2011).
20) Detection of spin-wave spin current in a magnetic insulator, Y. Kajiwara, S. Takahashi, S. Maekawa, and E. Saitoh, *IEEE Transaction on Magnetics* **47**, 1591-1594 (2011).
21) Electronic excitations around the substituted atom in $La_2Cu_{1-y}Ni_yO_4$ as seen via resonant inelastic x-ray scattering, K. Ishii, K. Tsutsui, K. Ikeuchi, I. Jarrige, J. Mizuki, H. Hiraka, K. Yamada, S. Maekawa, Y. Endoh, H. Ishii, and Y.Q.Cai, *Phys. Rev. B* **85**, 104509-1-104509-5 (2012).
22) Acoustic spin pumping: Direct generation of spin currents from sound waves in $Pt/Y_3Fe_5O_{12}$ hybrid structures, K. Uchida, H. Adachi, T. An, H. Nakayama, M. Toda, B. Hillebrands, S. Maekawa, and E. Saitoh, *J. Appl. Phys.* **111**, 153903-1-053903-8 (2012).

Invited Talks

1) Theory on pure spin current, S. Maekawa, *Intermag 2011*, Taipei, Taiwan (2011).
2) Are only phonons relevant to the long-range nature of the spin Seebeck effect?, H. Adachi, *Spin Caloritronics III*, Leiden, Netherlands (2011).
3) Spin current from mechanical motion, J. Ieda, *Spin Caloritronics III*, Leiden, Netherlands (2011).
4) Spin-wave, spin current and spin seebeck effect, S. Maekawa, *PM'11*, Poznan, Poland (2011).
5) Spin Seebeck effect and thermoelectric power generation by insulator, H. Adachi, *Recent Progress on Thermoelectric Materials and Modules*, Tokyo, Japan, (2011).
6) Conservation laws and spin motive force in magnetic nanostructures, S. Maekawa, *5th international workshop on Spin Current*, Sendai, Japan (2011).
7) Non-equilibrium magnons, spin current and spin Seebeck effect, S. Maekawa, *2nd International Workshop on Magnonics: From Fundamentals to Applications*, Recife, Brazil (2011).
8) Dynamics of Josephson-phase coupled with spin waves, M. Mori, *The 26th International Conference on Low Temperature Physics (LT26)*, Beijing, China (2011).
9) Conservation laws and spin motive force in magnetic nanostructures, S. Maekawa, *Moscow International Symposium on Magnetism*, Moscow, Russia (2011).
10) Theory of phonon-drag spin Seebeck effect, H. Adachi, *The 4th annual showcase of materials-allied research at The Ohio State University*, Ohio, USA (2011).
11) Influences of magnetic-fluctuation, resonance, and oscillation on Josephson current in superconductor/ferromagnet/superconductor junction, M. Mori, *Vortex matter in nanostructured superconductors (VORTEX VII)*, Rhodes, Greece (2011).
12) Thermopower in correlated electron systems revisited: non-monotonic temperature dependence, M. Mori, *ARW Workshop Hvar 2011*, Hvar, Croatia (2011).
13) Seebeck effect, spin Seebeck effect and spin-electronics, S. Maekawa, *The 2nd International Symposium on Hybrid Materials and Processing 2011*, Busan, Korea (2011).
14) Magnons, phonons, and spin Seebeck effect, S. Maekawa, *56th Annual Conference on Magnetism & Magnetic Materials*, Arizona, USA (2011).
15) Magnetic resonance appeared in ferromagnetic Josephson junction, M. Mori, *2011 Gordon Godfrey Workshop on Spins and Strong Correlations*, Sydney, Australia (2011).
16) Spin-motive force in magnetic nanostructures, S. Maekawa, *Joint Polish-Japanese Workshop on "Spintronics-from new materials to applications"*, Warsaw, Poland (2011).
17) Heat and spin, S. Maekawa, *FIRST-QS2C Workshop on "Eergent Phoenomena of Carrelated Materials"*, Okinawa, Japan (2011).
18) Theory on spin current generation, S. Maekawa, *SpinCaT conference*, Bonn, Germany (2012).
19) Phonon-driven spin Seebeck effect, H. Adachi, *2nd ASRC International Workshop on Magnetic materials and Nanotructures*, Tokai, Japan (2012).
20) Spin-Motive Force, S. Maekawa, *RIKEN-APW-APCTP Jpint Workshop "Recet trend in condensed matter physics"*, Wako, Japan (2012).
21) Heat and spin, S. Maekawa, *ILL Colloquium*, Grenoble, France (2012)
22) Magnons, spin current and spin Seebeck effect, S. Maekawa, *APS March Meeting*, Boston, USA (2012).
23) Spin-motive force and electric field effects, J. Ieda, *Mini workshop on electric field effect*, Sendai, Japan (2011).

Research Group for Molecular Spintronics

Papers

1) Interface properties of Ag and Au / graphene heterostructures studied by micro-raman spectroscopy, S. Entani, S. Sakai, Y. Matsumoto, H. Naramoto, T. Hao, and Y. Maeda, *Jpn. J. Appl. Phys.* **50**, 04DN03-1-04DN03-5 (2011).
2) Ab initio LC-DFT study of graphene, multilayer graphenes and graphite, P. V. Avramov, S. Sakai, S. Entani, Y. Matsumoto, and H. Naramoto, *Chem. Phys. Lett.* **508**, 86-89 (2011).
3) Effect of cotunneling and spin polarization on the large tunneling magnetoresistance effect in granular C_{60}-Co films, S. Sakai, S. Mitani, I. Sugai, K. Takanashi, Y. Matsumoto, S. Entani, H. Naramoto, P. Avramov, and Y. Maeda, *Phys. Rev. B* **83**, 174422-1-174422-6 (2011).
4) Multiplet scattering approach to XAS for Co-C_{60} Films, I. Hojo, Y. Matsumoto, T. Maruyama, S. Nagamatsu, S. Entani, S. Sakai, T. Konishi, and T. Fujikawa, *Photon Factory News* **29**, 20-25 (2011) (*in Japanese*).
5) Thermo-dynamical contours of electronic-vibrational spectra simulated using the statistical quantum–mechanical methods, V. Pomogaev, A. Pomogaeva,

P. Avramov, K. J. Jalkanen, and S. Kachin, *Theor. Chem. Acc*. **130**, 609-632 (2011).
6) Ferromagnetic interlayer coupling in C_{60}-Co compound / Ni bilayer structure, Y. Matsumoto, S. Sakai, S. Entani, Y. Takagi, T. Nakagawa, H. Naramoro, P. Avramov, and T. Yakoyama, *Chem. Phys. Lett*. **511**, 68-72 (2011).
7) Ion channeling study of epitaxy of iron based Heusler alloy films on Ge(111), Y. Maeda, K. Narumi, S. Sakai, Y. Terai, K. Hamaya, T. Sadoh, and M. Miyao, *Thin Solid Films* **519,** 8461-8467 (2011).
8) Determination of silicon vacancy in ion-beam synthesized β-FeSi2, Y. Maeda, T. Ichikawa, T. Jonishi, and K. Narumi, *Physics Procedia* **11**, 83-86 (2011).
9) Relative isomer abundance of fullerenes and carbon nanotubes correlates with kinetic stability, A. S. Fedorov, D. A. Fedorov, A. A. Kuzukov, P. V. Avramov, Y. Nishimura, S. Irle, and H. A. Witek, *Phys. Rev. Lett*. **107**, 175506-1-175506-5 (2011).
10) Local structures and magnetic properties of fullerene-Co systems studied by XAFS and XMCD analyses, I. Hojo, A. Koide, Y. Matsumoto, T. Maruyama, S. Nagamatsu, S. Entani, S. Sakai, and T. Fujikawa, *J. Electro. Spec. Relat. Phenom* **185**, 32-38 (2012).
11) Bias voltage dependence of tunneling magnetoresistance in granular C_{60}-Co films with current-perpendicular-to-plane geometry, S. Sakai, S. Mitani, Y. Matsumoto, S. Entani, P. Avramov, M. Ohtomo, H. Naramoto, and K. Takanashi, *J. Magn. Magn, Mater*. **324**, 1970-1974 (2012).
12) Precise control of single- and bi-layer graphene growths on epitaxial Ni(111) thin film, S. Entani, Y. Matsumoto, M. Ohtomo, P. V. Avramov, H. Naramoto, and S. Sakai, *J. Appl. Phys*. **111**, 064324-1-064324-6 (2012) (Press release 30th, May, 2012).
13) Structure determination of self-assembled monolayer on oxide surface by soft-X-ray standing wave, Y. Baba, A. Narita, T. Sekiguchi, I. Shimoyama, N. Hirao, S. Entani, and S. Sakai, *e-Journal of Surf. Sci. Nanotech*. **10**, 69-73 (2012).
14) Quasi-monochromatic pencil beam of laser-driven protons generated using a conical cavity target holder, M. Nishiuchi, A. S. Pirozhkov, H. Sasaki, K. Ogura, T. Esirkepov, T. Tanimoto, M. Kanasaki, A. Yogo, T. Hori, A. Sagisaka, Y. Fukuda, Y. Matsumoto, S. Entani, S. Sakai, C. Brenner, D. Neely, T. Yamauchi, S. V. Bulanov, and K. Kondo, *Physics of Plasmas* **19**, 030706-1-030706-4 (2012).

Invited Talks

1) Spin states of molecules and nanocarbons analyzed by X-ray magnetic dichroism spectroscopy, Y. Matsumoto, *Photon Factory Meeting*, Tsukuba, Japan (2012) (*in Japanese*).

Research Group for Mechanical Control of Materials and Spin Systems

Papers

1) Universality of the spin pumping in metallic bilayer Films, T. Yoshino, K. Ando, K. Harii, H. Nakayama, Y. Kajiwara and E. Saitoh, *Appl. Phys. Lett.* **98**, 132503-1-132503-3 (2011).
2) Inverse spin-Hall effect induced by spin pumping in metallic system, K. Ando, S. Takahashi, J. Ieda, Y. Kajiwara, H. Nakayama, T. Yoshino, K. Harii, Y. Fujikawa, M. Matsuo, S. Maekawa, and E. Saitoh, *J. Appl. Phys.* **109**, 103913-1-103913-3 (2011).
3) Spin pumping by parametrically excited exchange magnons, C. W. Sandweg, Y. Kajiwara, A. V. Chumak, A. A. Serga, V. I. Vasyuchka, M. B. Jungfleisch, E. Saitoh, and B. Hillebrands, *Phys. Rev. Lett.* **106**, 216601-1-216601-4 (2011).
4) Detection of spin-wave spin current in a magnetic insulator, Y. Kajiwara, S. Takahashi, S. Maekawa, and E. Saitoh, *IEEE Transaction on Magnetics* **47**, 1591-1594 (2011).
5) Spin current depolarization under high electric fields in undoped InGaAs, N. Okamoto, H. Kurebayashi, K. Harii, Y. Kajiwara, H. Beere, I. Farrer, T. Trypiniotis, K. Ando, D. A. Ritchie, C. H. W. Barnes, and E. Saitoh, *Appl. Phys. Lett.* **98**, 242104-1-242104-3 (2011).
6) Spin current generation due to mechanical rotation in the presence of impurity scattering, M. Matsuo, J. Ieda, E. Saitoh, and S. Maekawa, *Appl. Phys. Lett.* **98**, 242501-1-242501-3 (2011).
7) Frequency dependence of spin pumping in Pt/$Y_3Fe_5O_{12}$ Film, K. Harii, T. An, Y. Kajiwara, K. Ando, H. Nakayama, T. Yoshino, and E. Saitoh, *J. Appl. Phys.* **109**, 116105-1-116105-3 (2011).
8) Spin Seebeck effect in thin films of the Heusler compound Co_2MnSi, S. Bosu, Y. Sakuraba, K. Uchida, K. Saito, T. Ota, E. Saitoh, and K. Takanashi, *Phys. Rev. B* **83**, 224401-1-224401-6 (2011).
9) Electric detection of the spin-Seebeck effect in magnetic insulator in the presence of interface barrier, K. Uchida, T. Ota, Y. Kajiwara, H. Umezawa, H. Kawai, and E. Saitoh, *J. Phys.: Conf. Ser.* **303**, 012096-1-012096-4 (2011).
10) Electrically tunable spin injector free from the impedance mismatch problem, K. Ando, S. Takahashi, J. Ieda, H. Kurebayashi, T. Trypiniotis, C.H.W. Barnes, S. Maekawa, and E. Saitoh, *Nature materials* **10**, 655-659 (2011).
11) Spin-dependent inertial force and spin current in accelerating systems, M. Matsuo, J. Ieda, E. Saitoh, and S. Maekawa, *Phys. Rev. B* **84**, 104410-1-104410-9 (2011).
12) Nonlinear spin pumping induced by parametric excitation, K. Ando, T. An, E. Saitoh, *Appl. Phys. Lett.* **99**, 092510-1-092510-4 (2011).
13) Long-range spin Seebeck effect and acoustic spin pumping, K. Uchida, H. Adachi, T. An, T. Ota, M. Toda, B. Hillebrands, S. Maekawa, and E. Saitoh, *Nature materials* **10**, 737-741 (2011).
14) Spin pumping in polycrystalline magnetic insulator/metal Pt films, Y. Kajiwara, K. Ando, H. Nakayama, R. Takahashi, and E. Saitoh, *IEEE Transaction on Magnetics* **47**, 2739-2742 (2011).
15) Temporal evolution of inverse spin Hall effect voltage in a magnetic insulator-nonmagnetic metal structure, M. B. Jungfleisch, A. V. Chumak, V. I. Vasyuchka, A. A. Serga, B. Obry, H. Schultheiss, P. A. Beck, A.D. Karenowska, E. Saitoh, and B. Hillebrands, *Appl. Phys. Lett.* **99**, 182512-1-182512-3 (2011).
16) Surface-acoustic-wave-driven spin pumping in $Y_3Fe_5O_{12}$/Pt hybrid structures, K. Uchida, T. An, Y. Kajiwara, M. Toda, and E. Saitoh, *Appl. Phys. Lett.* **99**, 212501-1-212501-3 (2011).
17) Continuous generation of spinmotive force in a patterned ferromagnetic film, Y. Yamane, K. Sasage, T. An, K. Harii, J. Ohe, J. Ieda, S. E. Barnes, E. Saitoh, and S. Maekawa, *Phys. Rev. Lett.* **107**, 236602-1-236602-4 (2011).
18) Two-dimensional temperature mapping using spin-Seebeck insulator, K. Uchida, A. Kirihara, M. Ishida, R. Takahashi, and E. Saitoh, *Jpn. J. Appl. Phys. (Rapid Communication)* **50**, 120211-1-120211-3 (2011).
19) Strong Correlation among structural, electronic, and magnetic properties of $Sr_2Fe_{1+x}Mo_{1-x}O_6$ ($0<x<1$), K. Yoshida, S. Ikeuchi, H. Shimizu, S. Okayasu, and T. Suzuki, *J. Phys. Soc. Jpn.* **80**, 044716-1-044716-4 (2011).
20) Flux pinning properties of correlated pinning at low temperatures in ErBCO films with inclined columnar defects, S. Awaji, M. Namba, K. Watanabe, H. Kai, M. Mukaida, and S. Okayasu, *J. Appl. Phys.* **111**, 013914-1-013914-4 (2012).
21) X-ray detection capability of a $BaCl_2$ single crystal scintillator, M. Koshimizu, K. Onodera, F. Nishikido, R. Haruki, K. Shibuya, S. Kishimoto, and K. Asai, *J. Appl. Phys.* **111**, 024906-1-024906-5 (2012).
22) Fast scintillation detectors for high-energy X-ray region, S. Kishimoto, F. Nishikido, R. Haruki, K. Shibuya, and M. Koshimizu, *Hyperfine Interact.* **204**, 101-110 (2012).
23) All-oxide system for spin pumping, Z. Qiu,Y. kajiwara, K. Ando, Y. Fujikawa, K. Uchida, T. Tashiro, K. Harii, T. Yoshino, and E. Saitoh, *Appl. Phys. Lett.* **100**, 02240211-02240213 (2012).
24) Electroresistance effect in gold thin film induced by ionic liquid gated electric double layer, H. Nakayama, J. Ye T. Ohtani, Y. Fujikawa, K. Ando, Y. Iwasa, and E. Saitoh, *Appl. Phys. Express* **5**, 023002-1-023002-3 (2012).
25) Radiation effects on film formation and nanostructural changes of iron disilicide thin film, M. Sasase, H. Yamamoto, and S. Okayasu, *Nucl. Inst. Meth. Phys. Res. B* **272**, 318-321 (2012).
26) Observation of inverse spin-Hall effect in silicon, K. Ando and E. Saitoh, *Nature communications* **3**, 629-1-629-6 (2012).
27) Scaling fit of spin pumping in various ferromagnetic materials, T. Yoshino, K. Ando, Y. Kajiwara, H. Nakayama, and E. Saitoh, *J. Appl. Phys.* **111** 07C502-1-07C502-3 (2012).
28) Electrical determination of spin mixing conductance at metal/insulator interface using inverse spin-Hall effect, R. Takahashi, R. Iguchi, K. Ando, H. Nakayama, T. Yoshino, and E. Saitoh, *J. Appl. Phys.* **111**, 07C307-1-07C307-3 (2012).
29) Acoustic spin pumping: Direct generation of spin currents from sound waves in $Y_3Fe_5O_{12}$/Pt hybrid structures, K. Uchida, H. Adachi, T. An, H. Nakayama, M. Toda, B. Hillebrands, S. Maekawa, and E. Saitoh, *J. Appl. Phys.* **111**, 053903-1-053903-8 (2012).
30) Thermal artifact on the spin Seebeck effect in metallic thin films deposited on MgO substrates S. Bosu, Y. Sakuraba, K. Uchida, K. Saito, W, Kobayashi, E. Saitoh, and K. Takanashi, *J. Appl. Phys.* **111**, 07B106-1-07B106-3 (2012).

Books & Reviews

1) Progress in spin current science, E. Saitoh, *PARITY* **26**, No.1, 32-33 (2011) (*in Japanese*).
2) Spin injection in Mott insulator, E. Kajiwara, K. Ando, and E. Saitoh, *KOTAI BUTSURI* **46**, 115-164 (2011) (*in Japanese*).
3) A new application for electron spin: Spintronics in insulators, E. Saitoh, *PARITY* **26**, No.5, 48-51 (2011) (*in Japanese*).
4) E. Saitoh and K. Uchida, "Thermoelectric generation using Seebeck effect in insulators", Principle and Applications in Thermoelectoric Conversion Technology, CMS Press, 13-23 (2011).
5) Spintronics – a new role of spin in electronics, E. Saitoh, *OYO BUTSURI* **81**, 71-74 (2012) (*in Japanese*).

Invited Talks

1) Spin Seebeck effect in metallic materials, E. Saitoh, *SORST Symposium*, Tokyo, Japan (2011).
2) Spin current generation from metals and insulators, E. Saitoh, *International Symposium "Nanoscience and Quantum Physics 2011"*, Tokyo, Japan (2011).
3) Spintronics and spin current, E. Saitoh, *The 20th young forum for Advanced material science*, Funabashi, Japan (2011).
4) Spin current generation from insulators and metals, E.Saitoh, *The 3rd Scienceweb GCOE International Symposium*, Sendai, Japan (2011).
5) Spintronics in Mott Insulators, E. Saitoh, *PF Workshop*, Tsukuba, Japan (2011).
6) Spin pumping and spin Seebeck effects in insulators and metals, E. Saitoh, *2011 Materials Research Society Spring Meeting*, San Francisco, USA (2011).
7) Spin Hall effect and its application, E. Saitoh, *International Center for Quantum Materials (ICQM)*, Beijing, China (2011).
8) Spin current generation from magnetic dynamics and heat, E. Saitoh, *JSPS York-Tohoku Research Symposium on & "Magnetic Materials and Spintronics"*, York, UK (2011).
9) Spin current generation from magnetic dynamics and heat, E. Saitoh, *5th International Workshop on Spin Current*, Sendai, Japan (2011).
10) Spin current and heat: Development for new functional devices using spin

currents, E. Saitoh, *JST*, Tokyo, Japan (2011).
11) Physics and applications for spin current, E. Saitoh, *Science summer seminor*, Nagano, Japan (2011).
12) Spin Seebeck effect, E. Saitoh, *ASPIMATT school on "Advanced spintronic materials and transport phenomena"*, Diemerstein, Germany (2011).
13) Spin current generation using heat and magnetic dynamics, E. Saitoh, *2011 OSU Materials Week*, Ohio, USA (2011).
14) Fundamental physics on spin current, E. Saitoh, *JPS Autumn meeting 2011*, Toyama, Japan (2011).
15) Spin current generation using heat and magnetic dynamics E. Saitoh, *2011 International Conference on Solid State Devices and Materials (SSDM)*, Nagoya, Japan (2011).
16) Possibility of realization for electronic devices using spin current, E. Saitoh, *TECH Biz EXPO 2011*, Nagoya, Japan (2011).
17) Spin current generation using heat and magnetic dynamics, E. Saitoh, *Magnetism and Magnetic Materials Conference 2011*, Scottsdale, Arizona (2011).
18) Spin seebeck effect, E. Saitoh, *JSAP spintronics seminor*, Sendai, Japan (2011).
19) Spin current physics and application, E. Saitoh, *Joint Polish-Japanese Workshop: Spintronics-from new materials to applications*, Warsaw, Poland (2011).
20) Spin current physics and application, E. Saitoh, *The 7th International Conference on Advanced Materials and Devices (ICAMD2011)*, Jeju, Korea (2011) (*Plenary Talk*).
21) Spin current in metals and insulators, E. Saitoh, *The FIRST-QS2C Workshop on Emergent Phenomena of Correlated Materials*, Okinawa, Japan (2011).
22) Spin current and spintronics, E. Saitoh, *15th NAISTSeminor*, Nara, Japan (2011).
23) Spin current generation and utilization, E. Saitoh, *Spin Caloric Transport*, Bad Honnef, Germany (2012).
24) Spin current generation from heat and magnetic dynamics, E. Saitoh, *The 2nd ASRC International Workshop on Magnetic Materials and Nanostructures (JAEA)*, Tokai, Japan (2012).
25) Physics and applications on spin current, E. Saitoh, Sendai, Japan (2012).
26) Spin pumping and spin Seebeck effect, E. Saitoh, *American Physical Society March Meeting*, Boston, USA (2012).
27) Thermo – acoustic effect in spin current, E. Saitoh, *Japan Physical Society Annual Meeting*, Kobe, Japan (2012).

Research Group for Reactions Involving Heavy Nuclei

Papers

1) Effective radii of deuteron induced reactions, S. Hashimoto, M. Yahiro, K. Ogata, K. Minomo, and S. Chiba, *Phys. Rev. C* **83**, 054617-1-054617-11 (2011).
2) Systematic description of ^{6}Li(*n, n'*)*dα* reactions with the microscopic coupled-channels method, T. Matsumoto, D. Ichinkohorloo, Y. Hirabayashi, K. Katō, and S. Chiba, *Phys. Rev. C* **83**, 064611-1-064611-6 (2011).
3) In-beam γ -ray spectroscopy of ^{35}Mg and ^{33}Na, A. Gade, D. Bazin, B.A. Brown, C.M. Campbell, J.M. Cook, S. Ettenauer, T. Glasmacher, K.W. Kemper, S. McDaniel, A. Obertelli, T. Otsuka, A. Ratkiewicz, J.R. Terry, Y. Utsuno, and D. Weisshaar, *Phys. Rev. C* **83**, 044305-1-044305-5 (2011).
4) Dynamical model of surrogate reaction, Y. Aritomo, S. Chiba, and K. Nishio, *Phys. Rev. C* **84**, 024602-1-024602-10 (2011).
5) Spin-dependent observables in surrogate reactions, S. Chiba, O. Iwamoto, and Y. Aritomo, *Phys. Rev. C* **84**, 054602-1-054602-5 (2011).
6) Radiochemical study of sub-barrier fusion hindrance in the ^{19}F +^{209}Bi reaction, I. Nishinaka, Y. Kasamatsu, M. Tanikawa, S. Goto, and M. Asai, *Proc. Radiochim. Acta* **1**, 117-121 (2011).
7) Three-body model calculation of spin distribution in two-nucleon transfer reaction, K. Ogata, S. Hashimoto, and S. Chiba, *J. Nucl. Sci. Technol.* **48**, 1337-1342 (2011).
8) Fission of actinide nuclei with double Λ particles within the Skyrme-Hartree-Fock method, F. Minato and S. Chiba, *Nucl. Phys. A* **856**, *55-67* (2011).
9) Production and decay properties of ^{264}Hs and ^{265}Hs, N. Sato, H. Haba, T. Ichikawa, D. Kaji, Y. Kudou, K. Morimoto, K. Morita, K. Ozeki, T. Sumita, A. Yoneda, E. Ideguchi, H. Koura, A. Ozawa, T. Shinozuka, T. Yamaguchi, and A. Yoneda, *J. Phys. Soc. Jpn.* **80**, 094201-1-094201-7 (2011).
10) Isomeric states in ^{253}No and ^{253}Fm, S. Antalic, F.P. Hessberger, D. Ackermann, S. Heinz, S. Hofmann, Z. Kalaninova, B. Kindler, J. Khuyagbaatar, I. Kojouharov, P. Kuusiniemi, M. Leino, B. Lommel, R. Mann, K. Nishio, S. Saro, B. Streicher, B. Sulignano, and M. Venhart, *Eur. Phys. J. A* **47**, 62-1-62-12 (2011).
11) Covariance evaluation for actinide nuclear data in JENDL-4, O. Iwamoto, T. Nakagawa, S. Chiba, and N. Otuka, *J. Kor. Phys. Soc.* **59**, 1224-1229 (2011).
12) Self-consistent analyses of nuclear level structures, and nucleon interaction data of even-even Sn Isotopes, J.-Y. Lee, E.Sh. Soukhovitskij, Y. Kim, R. Capote, S. Chiba, and J.M. Quesada, *J. Kor. Phys. Soc.* **59**, 1019-1022 (2011).
13) Status of JENDL high energy file, Y. Watanabe, K. Kosako, S. Kunieda, S. Chiba, R. Fujimoto, H. Harada, M. Kawai, F. Maekawa, T. Murata, H. Nakashima, K. Niita, N. Shigyo, S. Shimakawa, N. Yamano, and T. Fukahori, *J. Kor. Phys. Soc.* **59**, 1040-1045 (2011).
14) JENDL-4.0: A new library for innovative nuclear energy systems, K. Shibata, O. Iwamoto, T. Nakagawa, N. Iwamoto, A. Ichihara, S. Kunieda, S. Chiba, and J. Katakura, *J. Kor. Phys. Soc.* **59**, 1046-1051 (2011).
15) Measurements of inelastic neutron scattering at 96 MeV from carbon, iron, yttrium and lead, A. Ohrn, C. Gustavsson, M. Blann, V. Blideanu, J. Blomgren, S. Chiba, H. Duarte, F. Haddad, C. Kalbach, J. Klug, A. Koning, C. Le brun, C. Lebrun, F. R. Lecolley, X. Ledoux, N. Marie-noury, P. Mermod, L. Nilsson, M. Osterlund, S. Pomp, A. Prokofiev, U. Tippawan, and Y. Watanabe, *J. Kor. Phys. Soc.* **59**, 1817-1820 (2011).
16) Neutron production in the lunar subsurface from alpha particles in galactic cosmic rays, S. Ota, S. Kobayashi, L. Sihver, N. Yamashita, and N. Hasebe, *Earth Planets Space* **63**, 25-35 (2011).
17) Charge resolution of CR-39 plastic nuclear track detectors for intermediate energy heavy ions, S. Ota, N. Yasuda, L. Sihver, S. Kodaira, M. Kurano, S. Naka, Y. Ideguchi, E. R. Benton, and N. Hasebe, *Nucl. Instr. Meth. B* **269**, 1382-1388 (2011).
18) Spin-polarization of radioactive ^{123}In$_{g.s.}$ by the tilted-foil method, Y. Hirayama, M. Mihara, Y.X. Watanabe, S.C. Jeong, N. Imai, K. Matsuta, H. Miyatake, T. Hashimoto, H. Ishiyama, S. Ichikawa, T. Ishii, T. Izumikawa, I. Katayama, H. Kawakami, I. Nishinaka, K. Nishio, H. Makii, S. Mitsuoka, S. Momota, A. Osa, Y. Otokawa, T.K. Sato, and Y. Wakabayashi, *Eur. Phys. J. A* **47**, 138-1-138-5 (2011).
19) Analysis of n+^{6}Li reactions in three-body model, D. Ichinkhorloo, T. Matsumoto, Y. Hirabayashi, K. Katō, and S. Chiba, *J. Nucl. Sci. Technol.* **48**, 1357-1360 (2011).
20) Shell structure of even-even nickel isotopes containing twenty to forty neutrons, O.V. Bespalova, I.N. Boboshin, V.V. Varloamov, T.A. Ermakova, B.S. Ishkhanov, A.A. Klimochkina, S.Yu. Komarov, H. Koura, E.A. Romanovsky, and T.I. Spasskaya, *Phys. Atom. Nucl.* **74**, 1521-1535 (2011).
21) Effects of nuclear orientation on fusion and fission process for reactions using ^{238}U target nucleus, K. Nishio, *J. Phys.*: *Conf. Ser.* **312**, 082007-1-082007-10 (2011).
22) Proton-proton phase shifts calculations in momentum space by a rigorous Coulomb treatment, S. Oryu, Y. Hiratsuka, S. Nishinohara, and S. Chiba, *J. Phys. G* **39**, 045101-1-045101-12 (2012).
23) Dynamical approach to heavy-ion induced fission using actinide target nuclei at energies around the Coulomb barrier, Y. Aritomo, K. Hagino, K. Nishio, and S. Chiba, *Phys. Rev. C* **85**, 044614-1-044614-15 (2012).
24) Production of ^{265}Sg in the ^{248}Cm(^{22}Ne, 5*n*)^{265}Sg reaction and decay properties of two isomeric states in ^{265}Sg, H. Haba, D. Kaji, Y. Kudou, K. Morimoto, K. Morita, K. Ozeki, R. Sakai, T. Sumita, A. Yoneda, Y. Kasamatsu, Y. Komori, A. Shinohara, H. Kikunaga, H. Kudo, K. Nishio, K. Ooe, N. Sato, and K. Tsukada, *Phys. Rev. C* **85**, 024611-1-024611-11 (2012).
25) High-spin spectrum of ^{24}Mg studied through multiparticle angular correlations, E. S. Diffenderfer, L. T. Baby, D. Santiago-Gonzalez, N. Ahsan, A. Rojas, A. Volya, I. Wiedenhover, A. H. Wuosmaa, M. P. Carpenter, R. V. F. Janssens, C. J. Lister, M. Devlin, D. G. Sarantites, L. G. Sobotka, Y. Utsuno, and M. Horoi, *Phys. Rev. C 85*, 034311-1-034311-17 (2012).
26) Tilted-foil technique for producing a spin-polarized radioactive isotope beam, Y. Hirayama, M. Mihara, Y. X. Watanabe, S. C. Jeong, H. Miyatake, S. Momota, T. Hashimoto, N. Imai, K. Matsuta, H. Ishiyama, S. Ichikawa, T. Ishii, T. Izumikawa, I. Katayama, H. Kawakami, H. Kawamura, I. Nishinaka, K. Nishio, H. Makii, S. Mitsuoka, A. Osa, Y. Otokawa, and T. K. Sato, *Eur. Phys. J. A* **48**, 54-1-54-10 (2012).

Books & Reviews

1) From my experience of monitoring environmental radiation levels after the Fukushima-Daiichi nuclear accident, S. Mitsuoka, *Nuclear Data News* **100**, 27-30 (2011) (*in Japanese*).
2) Recent study of nuclear masses—Report of RIBF-ULIC Symposium: Physics of Rare-RI Ring, H. Koura, *Nuclear Data News* **101**, 20-30 (2012) (*in Japanese*).
3) Nucleosynthesis in supernovae and neutrino oscillation, T. Suzuki, T. Yoshida, S. Chiba, and T. Kajino, *BUTSURI* **67**, 49-54 (2011) (*in Japanese*).
4) Surrogate method, S. Chiba, in *Soryushiron Kenkyu*, *Electronic Edition*, Vol. 10, No. 2 (2011).

Invited Talks

1) Nuclear orientation in fusion and synthesis of heavy element at sub-barrier energy, K. Nishio, *The 7th International Conference on Dynamic Aspects of Nuclear Fission*, Smolenice, Slovakia (2011).
2) Recent development in the shell model: shell evolution and methodology, Y. Utsuno, *ECT* Workshop "Nuclear Structure Seen through Ground-State Properties of Exotic Nuclei"*, Trento, Italy (2011).
3) Long-term needs for nuclear data development, S. Chiba, *Technical Meeting on Long-Term Needs for Nuclear Data Development*, Vienna, Austria (2011).
4) Current status of nuclear mass formulae, H. Koura, *RIKEN RIBF-ULIC-Symposium "Physics of Rare-RI Ring"*, Wako, Japan (2011).
5) Surrogate reaction and nuclear data research in the future, S. Chiba, *The 1st International Symposium on the Science with KoRIA*, Sejong, Korea (2011).
6) Fission research activity at JAEA, K. Nishio, *The 5th ASRC International Workshop "Perspectives in Nuclear Fission"*, Tokai, Japan (2012).
7) Surrogate research study at JAEA, S. Chiba, *The 5th ASRC International Workshop "Perspectives in Nuclear Fission"*, Tokai, Japan (2012).

Research Group for Superheavy Elements

Papers

1) Fluorido complex formation of element 104, rutherfordium (Rf), Y. Ishii, A. Toyoshima, K. Tsukada, M. Asai, Z. J. Li, Y. Nagame, S. Miyashita, T. Mori, H. Suganuma, H. Haba, S. Goto, H. Kudo, K. Akiyama, Y. Oura, A. Shinohara, M. Schädel, V. Pershina, and J. V. Kratz, *Bull. Chem. Soc. Jpn.* **84**, 903-911 (2011).
2) Production and decay properties of ^{264}Hs and ^{265}Hs, N. Sato, H. Haba, T. Ichikawa, D. Kaji, Y. Kudou, K. Morimoto, K. Morita, K. Ozeki, T. Sumita, A. Yoneda, E. Ideguchi, H. Koura, A. Ozawa, T. Shinozuka, T. Yamaguchi, and A. Yoshida, *J. Phys. Soc. Jpn.* **80**, 094201-1-094201-7 (2011).
3) Production and properties of transuranium elements, Y. Nagame and M. Hirata, *Radiochim. Acta* **99**, 377-393 (2011).
4) Spin-polarization of radioactive $^{123}In_{g.s.}$ by the tilted-foil method, Y. Hirayama, M. Mihara, Y.X. Watanabe, S.C. Jeong, N. Imai, K. Matsuta, H. Miyatake, T. Hashimoto, H. Ishiyama, S. Ichikawa, T. Ishii, T. Izumikawa, I. Katayama, H. Kawakami, I. Nishinaka, K. Nishio, H. Makii, S. Mitsuoka, S. Momota, A. Osa, Y. Otokawa, T.K. Sato, and Y. Wakabayashi, Eur. Phys. J. A **47**, 138-1-138-5 (2011).
5) Search for a 2-quasiparticle high-K isomer in ^{256}Rf, A. P. Robinson, T. L. Khoo, D. Seweryniak, I. Ahmad, M. Asai, B. B. Back, M. P. Carpenter, P. Chowdhury, C. N. Davids, J. Greene, P. T. Greenlees, K. Hauschild, A. Heinz, R.-D. Herzberg, R. V. F. Janssens, D. G. Jenkins, G. D. Jones, S. Ketelhut, F. G. Kondev, T. Lauritsen, C. J. Lister, A. Lopez-Martens, P. Marley, E. McCutchan, P. Papadakis, D. Peterson, J. Qian, D. Rostron, U. Shirwadkar, I. Stefanescu, S. K. Tandel, X. Wang, and S. Zhu, Phys. Rev. C **83**, 064311-1-064311-7 (2011).
6) The recoil transfer chamber. An interface to connect the physical preseparator TASCA with chemistry and counting setups, J. Even, J. Ballof, W. Brüchle, R. A. Buda, Ch.E. Düllmann, K. Eberhardt, A. Gorshkov, E. Gromm, D. Hild, E. Jäger, J. Khuyagbaatar, J.V. Kratz, J. Krier, D. Liebe, M. Mendel, D. Nayak, K. Opel, J.P. Omtvedt, P. Reichert, J. Runke, A. Sabelnikov, F. Samadani, M. Schädel, B. Schausten, N. Scheid, E. Schimpf, A. Semchenkov, P. Thörle-Pospiech, A. Toyoshima, A. Türler, V. Vicente Vilas, N. Wiehl, T. Wunderlich, and A. Yakushev, Nucl. Instrum. Methods A **638**, 157-164 (2011).
7) Radiochemical study of sub-barrier fusion hindrance in the $^{19}F+^{209}Bi$ reaction, I. Nishinaka, Y. Kasamatsu, M. Tanikawa, S. Goto, and M. Asai, *Proc. Radiochem. Acta* **1**, 117-122 (2011).
8) Solvent extraction of trivalent actinides with di(2-ethylhexyl) phosphoric acid, R. Takayama, K. Ooe, W. Yahagi, H. Fujisawa, Y. Komori, H. Kikunaga, T. Yoshimura, N. Takahashi, K. Takahisa, H. Haba, Y. Kudou Y. Ezaki, A. Toyoshima, M.Asai, Y. Nagame, T. Saito, T. Mitsugashira, and A. Shinohara, *Proc. Radiochem. Acta* **1**, 157-160 (2011).
9) Production of ^{265}Sg in the ^{248}Cm(^{22}Ne, 5*n*)^{265}Sg reaction and decay properties of two isomeric states in ^{265}Sg, H. Haba, D. Kaji, Y. Kudou, K. Morimoto, K. Morita, K. Ozeki, R. Sakai, T. Sumita, A. Yoneda, Y. Kasamatsu, Y. Komori, A. Shinohara, H. Kikunaga, H. Kudo, K. Nishio, K. Ooe, N. Sato, and K. Tsukada, *Phys. Rev. C* **85**, 024611-1-024611-11 (2012).
10) First experiment at TASCA towards x-ray fingerprinting of element 115 decay chains, U. Forsberg, P. Golubev, L.G. Sarmiento, J. Jeppsson, D. Rudolph, L.-L. Andersson, D. Ackermann, M. Asai, M. Block, K. Eberhardt, J. Even, Ch.E. Düllmann, J. Dvorak, J.M. Gates, K.E. Gregorich, R.-D. Herzberg, F.P. Heßberger, E. Jäger, J. Khuyagbaatar, I. Kojouharov, J.V. Kratz, J. Krier, N. Kurz, S. Lahiri, B. Lommel, M. Maiti, E. Merchán, J.P. Omtvedt, E. Parr, J. Runke, H. Schaffner, M. Schädel, and A. Yakushev, *Acta Phys. Pol. B* **43**, 305-311 (2012).
11) Sulfate complexation of element 104, Rf, in H_2SO_4/HNO_3 mixed solution, Z. J. Li, A. Toyoshima, M. Asai, K. Tsukada, T. K. Sato, N. Sato, T. Kikuchi, Y. Nagame, M. Schädel, V. Pershina, X. H. Liang, Y. Kasamatsu, Y. Komori, K. Ooe, A. Shinohara, S. Goto, H. Murayama, M. Murakami, H. Kudo, H. Haba, Y. Takeda, M. Nishikawa, A. Yokoyama, S. Ikarashi, K. Sueki, K. Akiyama, and J. V. Kratz, *Radiochim. Acta* **100**, 157-164 (2012).
12) Tilted-foil technique for producing a spin-polarized radioactive isotope beam, Y. Hirayama, M. Mihara, Y. X. Watanabe, S. C. Jeong, H. Miyatake, S. Momota, T. Hashimoto, N. Imai, K. Matsuta, H. Ishiyama, S. Ichikawa, T. Ishii, T. Izumikawa, I. Katayama, H. Kawakami, H. Kawamura, I. Nishinaka, K. Nishio, H. Makii, S. Mitsuoka, A. Osa, Y. Otokawa, and T. K. Sato, *Eur. Phys. J. A* **48**, 54-1-54-10 (2012).

Books & Reviews

1) Y. Nagame, M. Hirata, and H. Nakahara, "Production and Chemistry of Transuranium Elements", in "Handbook of Nuclear and Radiochemistry (Second Ed.)", edited by A. Vértes, S. Nágy, Z. Klencsar, R. G, Lovas, and F. Rösch, Springer, (Dordrecht), Vol. 2, pp. 817-875 (2011).

Invited Talks

1) Liquid phase experiments with the heaviest elements, Y. Nagame, *The 4th International Conference on the Chemistry and Physics of the Transactinide Elements (TAN11)*, Sochi, Russia (2011).
2) Chemistry and physics of (super-)heavy elements, M. Schädel, *Summer School on Actinide Science and Applications 2011*, Karlsruhe, Germany (2011).

Research Group for Actinide Materials Science

Papers

1) Properties of ferromagnetic superconductors, D. Aoki, F. Hardy, A. Miyake, V. Taufour, T.D. Matsuda, and J. Flouquet, *C. R. Physique* **12**, 573-583 (2011).
2 Pressure evolution of the magnetic field induced ferromagnetic fluctuation through the pseudo-metamagnetism of $CeRu_2Si_2$, D. Aoki, C. Paulsen, T.D. Matsuda, L. Malone, G. Knebel, P. Haen, P. Lejay, R. Settai, Y. Ōnuki, and J. Flouquet, *J. Phys. Soc. Jpn.* **80**, 053702-1-053702-4 (2011).
3) Superconductivity reinforced by magnetic field and the magnetic instability in uranium ferromagnets, D. Aoki, T.D. Matsuda, F. Hardy, C. Meingast, V. Taufour, E. Hassinger, I. Sheikin, C. Paulsen, G. Knebel, H. Kotegawa, and J. Flouquet, *J. Phys. Soc. Jpn.* **80**, *Suppl. A*, SA008-1- SA008-6 (2011).
4) Ferromagnetic Quantum Critical Endpoint in UCoAl, D. Aoki, T. Combier, V. Taufour, T.D. Matsuda, G. Knebel, H. Kotegawa, and J. Flouquet, *J. Phys. Soc. Jpn.* **80**, 094711-1-094711-10 (2011).
5) ^{237}Np nuclear relaxation rate in heavy fermion superconductor $NpPd_5Al_2$, H. Chudo, Y. Tokunaga, S. Kambe, H. Sakai, Y. Haga, T. Matsuda, Y. Ōnuki, H. Yasuoka, D. Aoki, Y. Homma, and R. Walstedt, *Phys. Rev. B* **84**, 094402-1-094402-5 (2011).
6) Electronic structure of heavy Fermion uranium compounds studied by core-level photoelectron spectroscopy, S.-I. Fujimori, T. Ohkochi, I. Kawasaki, A. Yasui, Y. Takeda, T. Okane, Y. Saitoh, A. Fujimori, H. Yamagami, Y. Haga, E. Yamamoto, Y. Tokiwa, S. Ikeda, T. Sugai, H. Ohkuni, N. Kimura, and Y. Ōnuki, *J. Phys. Soc. Jpn.* **81**, 014703-1-014703-9 (2011).
7) Crystal structure and physical properties of trigonal $NpGa_3$ and Np_3Ga_{11}, Y. Haga, D. Aoki, Y. Homma, T.D. Matsuda, S. Ikeda, H. Sakai, E. Yamamoto, A. Nakamura, Y. Shiokawa, and Y. Ōnuki, *J. Phys. Soc. Jpn.* **80**, *Suppl. A*, SA109-1- SA109-3 (2011).
8) Possible long-periodic magnetic atructure in $SmPb_3$, T.U. Ito, W. Higemoto, K. Ninomiya, A. Amato, T. Sugai, Y. Haga, and H.S. Suzuki, *J. Phys. Soc. Jpn.* **80**, *Suppl. A*, SA075-1- SA075-3 (2011).
9) T-dependent nuclear hyperfine coupling at the In site in $CeIrIn_5$, S. Kambe, H. Sakai, Y. Tokunaga, T.D. Matsuda, Y. Haga, T. Takeuchi, Y. Ōnuki, and R.E. Walstedt, *J. Phys. Soc. Jpn.* **80**, *Suppl. A*, SA009-1- SA009-3 (2011).
10) Band structure and Fermi surface of URu_2Si_2 studied by soft x-ray angle-resolved photoemission spectroscopy, I. Kawasaki, S.-I. Fujimori, Y. Takeda, T. Okane, A. Yasui, Y. Saitoh, H. Yamagami, Y. Haga, E. Yamamoto, and Y. Ōnuki, *Phys. Rev. B* **83**, 235121-1-235121-6 (2011).
11) Pressure-induced structural phase transitions in UIr, H. Kotegawa, S. Araki, T. Akazawa, A. Hori, Y. Irie, S. Fukushima, H. Hidaka, T. Kobayashi, K. Takeda, Y. Ohishi, K. Murata, E. Yamamoto, S. Ikeda, Y. Haga, R. Settai, and Y. Ōnuki, *Phys. Rev. B* **84**, 054524-1-054524-5 (2011).
12) Evidence for spin-glass state in nonmagnetic atom disorder compound Pr_2AgIn_3, D.X. Li, T. Yamamura, K. Yubuta, S. Nimori, Y. Haga, and T. Shikama, *J. Phys.: Conf. Ser.* **320**, 012041-1-012041-6 (2011).
13) Thermoelectric evidence for high-field anomalies in the hidden order phase of URu_2Si_2, L. Malone, T.D. Matsuda, A. Antunes, G. Knebel, V. Taufour, D. Aoki, K. Behnia, C. Proust, and J. Flouquet, *Phys. Rev. B* **83**, 245117-1-245117-5 (2011).
14) Details of sample dependence and transport properties of URu_2Si_2, T.D. Matsuda, E. Hassinger, D. Aoki, V. Taufour, G. Knebel, N. Tateiwa, E. Yamamoto, Y. Haga, Y. Ōnuki, Z. Fisk, and J. Flouquet, *J. Phys. Soc. Jpn.* **80**, 114710-1-114710-10 (2011).
15) Detailed characterization of U-Co binary compounds, T.D. Matsuda, T. Sugai, Y. Haga, E. Yamamoto, and Y. Ōnuki, *J. Phys. Soc. Jpn.* **80**, *Suppl. A*, SA101-1- SA101-3 (2011).
16) ^{9}Be-NMR spin-lattice relaxation rate in heavy-fermion superconductor UBe_{13}, K. Morita, Y. Hara, Z. Sakano, H. Kotegawa, H. Tou, Y. Haga, and Y. Ōnuki, *J. Phys. Soc. Jpn.* **80**, *Suppl. A*, SA099-1- SA099-3 (2011).
17) Magnetic properties of barium uranate $Ba_3U_2O_7$, A. Nakamura, Y. Doi, and Y. Hinatsu, *J. Sol. State Chem.* **184**, 531–535 (2011).
18) Strong longitudinal magnetic fluctuations near critical end point in UCoAl: A ^{59}Co-NMR study, H. Nohara, H. Kotegawa, H. Tou, T.D. Matsuda, E. Yamamoto, Y. Haga, Z. Fisk, Y. Ōnuki, D. Aoki, and J. Flouquet, *J. Phys. Soc. Jpn.* **80**, 093707-1-093707-4 (2011).
19) Characteristic heavy fermion properties in $YbCu_2Si_2$ and YbT_2Zn_{20} (T : Co, Rh, Ir), Y. Ōnuki, S. Yasui, M. Matsushita, S. Yoshiuchi, M. Ohya, Y. Hirose, N.D. Dung, F. Honda, T. Takeuchi, R. Settai, K. Sugiyama, E. Yamamoto, T.D. Matsuda, Y. Haga, T. Tanaka, Y. Kubo, and H. Harima, *J. Phys. Soc. Jpn.* **80**, *Suppl. A*, SA003-1- SA003-6 (2011).
20) High field magnetoresistance and de Haas-van Alphen effect in $LaRu_2Al_{10}$, M. Sakoda, S. Tanaka, E. Matsuoka, H. Sugawara, H. Harima, F. Honda, R. Settai, Y. Ōnuki, T.D. Matsuda, and Y. Haga, *J. Phys. Soc. Jpn.* **80**, 084716-1-084716-5 (2011).
21) Maki parameter and upper critical field of the heavy-Fermion superconductor UBe_{13}, Y. Shimizu, Y. Ikeda, T. Wakabayashi, Y. Haga, K. Tenya, H. Hidaka, T. Yanagisawa, and H. Amitsuka, *J. Phys. Soc. Jpn.* **80**, 093701-1-093701-4 (2011).
22) Specific heat and magnetization studies of the superconducting mixed state of UBe_{13}, Y. Shimizu, Y. Ikeda, T. Wakabayashi, K. Tenya, Y. Haga, H. Hidaka, T. Yanagisawa, and H. Amitsuka, *J. Phys. Soc. Jpn.* **80**, *Suppl. A*, SA100-1- SA100-3 (2011).
23) Magnetic-field-induced metallic state in β-US_2, K. Sugiyama, Y. Hirose, K. Enoki, S. Ikeda, E. Yamamoto, N. Tateiwa, Y. Haga, T. Kida, M. Hagiwara, K. Kindo, F. Honda, R. Settai, and Y. Ōnuki, *J. Phys. Soc. Jpn.* **80**, *Suppl. A*, SA104-1- SA104-3 (2011).
24) Non-magnetic to magnetic transition under high pressure in narrow-gap semiconductor β-US_2, N. Tateiwa, Y. Haga, H. Sakai, S. Ikeda, T.D. Matsuda, E. Yamamoto, and Y. Ōnuki, *J. Phys. Soc. Jpn.* **80**, *Suppl. A*, SA103-1- SA103-3 (2011).
25) Miniature ceramic-anvil high-pressure cell for magnetic measurements in a commercial superconducting quantum interference device magnetometer, N. Tateiwa, Y. Haga, Z. Fisk, and Y. Ōnuki, *Rev. Sci. Instrum.* **82**, 053906-1-053906-8 (2011).
26) Ultrasonic measurements on the cage-structured clathrate compound $U_3Pd_{20}Si_6$, T. Yanagisawa, N. Tateiwa, T. Mayama, H. Saito, H. Hidaka, H. Amitsuka, Y. Haga, Y. Nemoto, and T. Goto, *J. Phys. Soc. Jpn.* **80**, *Suppl. A*, SA105-1- SA105-3 (2011).

27) Electronic structure of $YbCu_2Ge_2$ studied by soft x-ray angle-resolved photoemission spectroscopy, A. Yasui, S.-I. Fujimori, I. Kawasaki, T. Okane, Y. Takeda, Y. Saitoh, H. Yamagami, A. Sekiyama, R. Settai, T. Matsuda, Y. Haga, and Y. Ōnuki, *Phys. Rev. B* **84**, 195121-1-195121-6 (2011).
28) Ultrahigh-resolution laser photoemission study of URu_2Si_2 across the hidden-order transition, R. Yoshida, Y. Nakamura, M. Fukui, Y. Haga, E. Yamamoto, Y. Ōnuki, M. Okawa, S. Shin, M. Hirai, Y. Muraoka, and T. Yokoya, *J. Phys. Chem. Solid*. **72**, 580–581 (2011).
29) Electrical and magnetic properties of quasicrystal approximants RCd_6 (R: Rare Earth), A. Mori, H. Ota, S. Yoshiuchi, K. Iwakawa, Y. Taga, Y. Hirose, T. Takeuchi, E. Yamamoto, Y. Haga, F. Honda, R. Settai, and Y. Ōnuki, *J. Phys. Soc. Jpn.* **81**, 024720-1-024720-10 (2012).
30) Strong correlation between anomalous quasiparticle scattering and unconventional superconductivity in the hidden-order phase of URu_2Si_2, N. Tateiwa, T. Matsuda, Y. Ōnuki, Y. Haga, and Z. Fisk, *Phys. Rev. B* **85**, 054516-1-054516-5 (2012).

Books & Reviews
1) Miniature ceramic anvil high-pressure cell (mCAC) for magnetic measurements, N. Tateiwa and Y. Haga, *KOTAI BUTSURI* **46**, 791-799 (2011) (*in Japanese*).

Invited Talks
1) Unconventional superconducting characteristics of heavy fermion actinide superconductors, Y. Haga, *Heavy Fermion Physics: Perspective and Outlook*, Beijing, China (2012).
2) Strong correlation between anomalous quasiparticle scattering and unconventional superconductivity in hidden order phase of URu_2Si_2, N. Tateiwa, *Heavy Fermion Physics: Perspective and Outlook*, Beijing, China (2012).

Research Group for Condensed Matter Physics of Heavy Element Systems

Papers
1) NMR determination of noncollinear antiferromagnetic structure in $TbCoGa_5$, Y. Tokunaga, Y. Saito, H. Sakai, S. Kambe, N. Sanada, R. Watanuki, K. Suzuki, Y. Kawasaki, and Y. Kishimoto, *Phys. Rev. B* **84**, 214403-1-214403-7 (2011).
2) μSR evidence of nonmagnetic order and ^{141}Pr hyperfine-enhanced nuclear magnetism in the Cubic Γ_3 ground doublet system $PrTi_2Al_{20}$, T. U. Ito, W. Higemoto, K. Ninomiya, H. Luetkens, C. Baines, A. Sakai, and S. Nakatsuji, *J. Phys. Soc. Jpn.* **80**, 113703-1-113703-4 (2011).
3) Magnetic-field-induced enhancements of nuclear spin-lattice relaxation rates in the heavy-fermion superconductor $CeCoIn_5$ using ^{59}Co nuclear magnetic resonance, H. Sakai, S. E. Brown, S.-H. Baek, F. Ronning, E. D. Bauer, and J. D. Thompson, *Phys. Rev. Lett.* **107**, 137001-1-137001-4 (2011).
4) Li(Zn,Mn)As as a new generation ferromagnet based on a I-II-V semiconductor, Z. Deng, C. Q. Jin, Q. Q. Liu, X. C. Wang, J. L. Zhu, S. M. Feng, L. C. Chen, R. C. Yu, C. Arguello, T. Goko, Fanlong Ning, Jinsong Zhang, Yayu Wang, A. A. Aczel, T. Munsie, T. J. Williams, G. M. Luke, T. Kakeshita, S. Uchida, W. Higemoto, T. U. Ito, Bo Gu, S. Maekawa, G. D. Morris, and Y. J. Uemura, *Nature Communications* **2**, 422 (2011).
5) ^{237}Np nuclear relaxation rate in heavy fermion superconductor $NpPd_5Al_2$, H. Chudo, Y. Tokunaga, S. Kambe, H. Sakai, Y. Haga, T. D. Matsuda, Y. Ōnuki, H. Yasuoka, D. Aoki and Y. Homma, and R. E. Walstedt, *Phys. Rev. B* **84**, 094402-1-094402-5 (2011).
6) Absence of pure quadrupole ordering in $SmSn_3$: Dipole-dipole and quadrupole-quadrupole interactions in Sm-based compounds, T. U. Ito, W. Higemoto, K. Ninomiya, and H. S. Suzuki, *Phys. Rev. B* **84**, 064411-1-064411-5 (2011).
7) Introduction of the research group for condensed matter physics in heavy elements system in ASRC, S. Kambe, "MESON" (Society of Muon and Meson Science of Japan) **34**, 17-22 (2011) (*in Japanese*).
8) Stabilization of commensurate antiferromagnetism in $CePt_2In_7$ by Pressure Up to 2.4 GPa: ^{115}In NMR and NQR under zero field, H. Sakai, Y. Tokunaga, S. Kambe, H.-O. Lee, V. A. Sidorov, P. H. Tobash, F. Ronning, E. D. Bauer, and J. D. Thompson, *Phys. Rev. B* **83**, 140408-1 140408-4(R) (2011).
9) Electronic inhomogeneity in a Kondo lattice, E. D. Bauer, Y.-f. Yang, C. Capan, R. R. Urbano, C. F. Miclea, H. Sakai, F. Ronning, M. J. Graf, A. V. Balatsky, R. Movshovich, A. D. Bianchi, A. P. Reyes, P. L. Kuhns, J. D. Thompson, and Z. Fisk, *Proceedings of the National Academy of Sciences of the United States of America* **108**, 6857-1-6857-5 (2011).
10) Incommensurate-to-commensurate magnetic phase transition in $SmIn_3$ observed by muon spin relaxation, T. U. Ito, W. Higemoto, K. Ninomiya, L. Hubertus, T. Sugai, Y. Haga, and H. S. Suzuki, *J. Phys. Soc. Jpn.* **80**, 033710-1-033710-4 (2011).
11) Suppression of time-reversal symmetry breaking superconductivity in $Pr(Os_{1-x}Ru_x)_4Sb_{12}$ and $Pr_{1-y}La_yOs_4Sb_{12}$, L. Shu, W. Higemoto, Y. Aoki, A. D. Hillier, K. Ohishi, K. Ishida, R. Kadono, A. Koda, O. O. Bernal, D. E. MacLaughlin, Y. Tunashima, Y. Yonezawa, S. Sanada, D. Kikuchi, H. Sato, H. Sugawara, T. U. Ito, and M. B. Maple, *Phys. Rev. B* **83**, 10050-1-100504-4(R) (2011).
12) Possible long-periodic magnetic structure in $SmPb_3$, T. U. Ito, W. Higemoto, K. Ninomiya, A. Amato, T. Sugai, Y. Haga, and H. S. Suzuki, *J. Phys. Soc. Jpn.* **80**, *Suppl. A*, SA075-1-075-3 (2011).
13) Dilute La-substitutions in $CeRhIn_5$ studied by means of NMR/NQR techniques, H. Sakai, N. Kurita, C. F. Miclea, R. Movshovich, H.-O. Lee, F. Ronning, E. D. Bauer, and J. D. Thompson, *J. Phys. Soc. Jpn.* **80**, *Suppl. A*, SA059-1-059-3 (2011).
14) *T*-dependent nuclear hyperfine coupling at the In site in $CeIrIn_5$, S. Kambe, H. Sakai, Y. Tokunaga, T.D. Matsuda, Y. Haga, T. Takeuchi, Y. Ōnuki, and R.E. Walstedt, *J. Phys. Soc. Jpn.* **80**, *Suppl. A*, SA009-1-009-3 (2011).
15) Non-magnetic to magnetic transition under high pressure in narrow-gap semiconductor β-US_2, N. Tateiwa, Y. Haga, H. Sakai, S. Ikeda, T.D. Matsuda, E. Yamamoto, and Y. Ōnuki, *J. Phys. Soc. Jpn.* **80**, *Suppl. A*, SA103-1-103-3 (2011).
16) Crystal structure and physical properties of trigonal $NpGa_3$ and Np_3Ga_{11}, Y. Haga, D. Aoki, Y. Homma, T. D. Matsuda, S. Ikeda, H. Sakai, E. Yamamoto, A. Nakamura, Y. Shiokawa, and Y. Ōnuki, *J. Phys. Soc. Jpn.* **80**, *Suppl. A*, SA109-1-109-3 (2011).
17) NMR study on AmO_2: comparison with UO_2 and NpO_2, Y. Tokunaga, T. Nishi, S. Kambe, M. Nakada, Y. Homma, H. Sakai, and H. Chudo, *J. Phys. Soc. Jpn.* **80**, *Suppl. A*, SA110-1-110-3 (2011).
18) Present situation of radioactivity measurements, K. Ninomiya, *Web. Site of Science Council of Japan* (2011).
19) Quasi-one-dimensional spin dynamics in LiV_2O_4: one-to-three-fimensional crossover as a possible origin of heavy Fermion state, R. Kadono, A. Koda, W. Higemoto, K. Ohishi, H. Ueda, C. Urano, S.-i Kondo, M. Nohara, and H. Takagi, *J. Phys. Soc. Jpn.* **81**, 014709-1-014709-4 (2012).

Invited Talks
1) Anisotropy of spin fluctuations in the heavy Fermion systems: Nuclear magnetic resonance study, H. Sakai, *TOKIMEKI2011 International Workshop on Heavy Fermions*, Osaka, Japan, (2011).
2) Ligand and actinide NMR studies in actinide oxides and intermetallic compounds, S. Kambe, *American Chemical Society Fall Meeting*, Denver, USA (2011).
3) NMR studies in actinide dioxides, Y. Tokunaga, *6th Workshop on Speciation, Techniques, and Facilities for Radioactive Materials at Synchrotron Light Sources and Other Quantum Beam Sources (AnXAS2011)*, Hyogo, Japan (2011).
4) Solid-state NMR study of actinide dioxides, Y. Tokunaga, *MRS Spring Meeting*, San-Francisco, USA (2012).
5) Spin fluctuation, orbital states and non-conventional superconductivity in actinides compounds, S. Kambe, *MRS Spring Meeting*, San-Francisco, USA (2012).
6) No-collinear antiferromagnetic structure in $TbCoGa_5$, Y. Tokunaga, *The 3rd ASRC International Workshop*, Grenoble, France (2012).
7) Our recent progress of NMR measurements under extreme condition in our research activity in ASRC-JAEA, H. Sakai, *The 3rd ASRC International Workshop*, Grenoble, France (2012).

Research Group for Hadron Physics

Papers
1) Identified charged hadron production in $p+p$ collisions at $\sqrt{s}$=200 and 62.4 GeV, A. Adare, K. Imai, S. Sato, K. Tanida et al., *Phys. Rev. C* **83**, 064903-1-064903-29 (2011).
2) Azimuthal correlations of electrons from heavy flavor decay with hadrons in $p+p$ and Au+Au collisions at $\sqrt{s_{NN}}$=200 GeV, A. Adare, K. Imai, K. Tanida, et al., *Phys. Rev. C* **83**, 044912-1-044912-16 (2011).
3) Measurement of neutral mesons in $p+p$ collisions at $\sqrt{s}$=200 GeV and scaling properties of hadron production, A. Adare, K. Imai, S. Sato, K. Tanida, et al., *Phys. Rev. D* **83**, 052004-1-052004-26 (2011).
4) Event structure and double helicity asymmetry in jet production from polarized $p+p$ collisions at $\sqrt{s}$=200 GeV, A. Adare, K. Imai, S. Sato, K. Tanida, et al., *Phys. Rev. D* **84**, 012006-1-012006-16 (2011).
5) Suppression of away-side jet fragments with respect to the reaction plane in Au+Au collisions at $\sqrt{s_{NN}}$=200 GeV, A. Adare, K. Imai, K. Tanida, et al., *Phys. Rev. C* **84**, 024904-1-024904-12 (2011).
6) Production of omega meson in $p+p$, d+Au, Cu+Cu, and Au+Au collisions at $\sqrt{s_{NN}}$=200 GeV, A. Adare, K. Imai, S. Sato, K. Tanida, et al., *Phys. Rev. C* **84**, 044902-1-044902-11 (2011).
7) Cold nuclear matter effects on J/psi yields as a function of rapidity and nuclear geometry in d+A collisions at $\sqrt{s_{NN}}$=200 GeV, A. Adare, K. Imai, K. Tanida, et al., *Phys. Rev. Lett.* **107**, 142301-1-142301-7 (2011).
8) Heavy-quark production in $p+p$ and energy loss and flow of heavy quarks in Au+Au collisions at $\sqrt{s_{NN}}$ =200 GeV, A. Adare, K. Imai, S. Sato, K. Tanida, et al., *Phys. Rev. C* **84**, 044905-1-044905-42 (2011).
9) Suppression of back-to back hadron pairs at forward rapidity in d+Au collisions at $\sqrt{s_{NN}}$ =200 GeV, A. Adare, K. Imai, K. Tanida, et al., *Phys. Rev. Lett.* **107**, 172301-1-172301-7 (2011).
10) Multi-antikaonic nuclei and in-medium kaon properties in dense matter, T. Muto, T. Maruyama, and T. Tatsumi, *J. Phys.: Conf. Ser.* **312**, 022018-1-022018-6 (2011).
11) Liquid-gas mixed phase in nuclear matter at finite temperature, T. Maruyama and T. Tatsumi, *J. Phys.: Conf. Ser*. **312**, 042015-1-042015-6 (2011).
12) Pasta structures of quark-hadron phase transition in proto-neutron stars, N. Yasutake, T. Maruyama, and T. Tatsumi. *J. Phys.: Conf. Ser.* **312**, 042027-1-042027-6 (2011).
13) Effect of Λ(1405) on the structure of multi-antikaonic nuclei, T. Muto, T. Maruyama, and T. Tatsumi, *AIP Conf. Proc.* **1374**, 197-200 (2011).
14) J-PARC facilities and physics, S. Sato, *Nucl. Phys.* A **862**, 238-243 (2011).
15) CANGAROO-III observation of TeV gamma rays from the unidentified gamma-ray source HESS J1614-518, T. Mizukami, R. Kiuchi, et al., *Astrophys. J*. **740**, 78-1-78-9 (2011).
16) J-PARC Status, Nuclear and Particle Physics, S. Sato, *AIP Conf. Proc*. **1336**, 560-564 (2011).
17) J-PARC and its prospect of particle and nuclear physics, K. Imai, *AIP Conf. Proc*. **1342**, 32-36 (2011).

18) Heavy ion microbeam system for cell irradiation at Kyoto University, M. Nakamura, K. Imai, M. Hirose, H. Matsumoto, M. Tosaki, D. Ohsawa, S. Makino, *Nucl. Instr. Meth. Phys. Res. B* **269**, 3153-3157 (2011).
19) Spin-density matrix elements for $\gamma p \rightarrow K^{*0}\Sigma^{+}$ at E_{γ}=1.85-3.0 GeV with evidence for the κ(800) meson exchange., S.H. Hwang, K. Hicks, K. Imai, et al., *Phys. Rev. Lett*. **108**, 092001-1- 092001-5 (2012).
20) Searches for very high energy gamma rays from blazars with CANGAROO-III telescope in 2005-2009, Y. Mizumura, R. Kiuchi, et al., *Astropart. Phys*. **35**, 563-572 (2012).
21) Development of a tracking detector system with multichannel scintillation fibers and PPD, R. Honda, S. Callier, S. Hasegawa, M. Ieiri, Y. Matsumoto, K. Miwa, I. Nakamura, L. Raux, C. DeLaTaille, M. Tanaka, T. Uchida, and K. Yoshimura, *Nucl. Instr. Meth. Phys. Res. A*, in press.
22) Search for θ^{+} via the pion induced reaction at J-PARC : J-PARC E19, K. Shirotori, R. Honda, K. Imai, H. Sako, S. Sato, Sugimura, et al., *Few-Body Systems*, in press.

Invited Talks
1) Strangeness nuclear physics at J-PARC, K. Imai, *Hadron physics meeting*, Pohang, Korea (2011).
2) Hadron Physics at J-PARC, K. Imai, *ECT Workshop on Strange Hadronic Matter*, Trento, Italy (2011).
3) Search for H-dibaryon at J-PARC, S. Sato, *ECT Workshop on Strange Hadronic Matter*, Trento, Italy (2011).
4) Experimental investigation of baryon-baryon interaction through Sigma-p scattering at J-PARC, R. Honda, *8th Postgraduate Academic Forum of Beihang University*, Beijing, China (2011).
5) Search for θ via the pion induced reaction at J-PARC: J-PARC E19, K.Shirotori, *The Fifth Asia-Pacific Conference on Few-Body Problems in Physics 2011 (APBF2011)*, Seoul, Korea (2011).
6) Search for θ pentaquark baryon at the J-PARC K1.8 beam line: First result and current status, K. Shirotori, *Hadron Physics Meeting (Strangeness Physics at J-PARC)*, Pohang, Korea (2011)
7) Status of E03 and E07, K. Tanida, *Korea-Japan workshop on nuclear and hadron physics at J-PARC*, Seoul, Korea (2011).
8) What is the charmed analog of Lambda(1405)?, K. Tanida, *The fifth Asia-Pacific Conference on Few-Body Problems in Physics 2011 (APFB2011)*, Seoul, Korea (2011).
9) Three-dimensional calculation of inhomogeneous structure in low-density nuclear matter, M. Okamoto, *XVth Research Workshop on Nucleation Theory and Applications*, Dubna, Russia (2011).
10) Overview of spin physics results from PHENIX experiment, K. Tanida for *the* PHENIX collaboration, *The 4th International Workshop of High Energy Physics in the LHC Era*, Valparaiso, Chile (2012).

Research Group for Bioactinide

Papers
1) Accumulation of Co in yeast cells under metabolically active condition -implication for role of yeast in migration of radioactive Co-, N. Kozai, T. Ohnuki, F. Sakamoto, Y. Suzuki, K. Tanaka, H. Iefuji, and T. Sakai, *J. Nucl. Sci. Technol*., **48**, 1206-1213 (2011).
2) Behavior of paramecium sp. in solutions containing Sr and Pb: Do paramecium sp. alter chemical forms of those met, N. Kozai, T. Ohnuki, M. Koka, T. Sato, and T. Kamiya, *Nucl. Instr. Meth. Phys. Res. B* **269**, 2393-2398 (2011).
3) Specific sorption behavior of actinoids on biogenic Mn oxide, K. Tanaka, Y. Tani, and T. Ohnuki, *Chem. Lett*. **40**, 806-807 (2011).
4) Interactions of the rare earth elements - desferrioxamine B complexes with *Pseudomonas fluorescens* and g-Al_2O_3, T. Ohnuki and T. Yoshida, *Chem. Lett*. **41**, 98-100 (2011).
5) Local area distribution of fallout radionuclides from Fukushima Daiichi Nuclear Power Plant by autoradiography analysis, F. Sakamoto, T. Ohnuki, N. Kozai, S. Igarashi, S. Yamasaki, Z. Yoshida, and S. Tanaka, *Trans. Atomic Energy Soc. Japan* **11**, 1-7 (2012) (*in Japanese*) .

Invited Talks
1) Biotransformation of rare earth elements, T. Ohnuki, *Goldschmidt Conference 2011*, Prague, Czech Republic (2011).

Research Group for Radiation and Biomolecular Science

Papers
1) Pulse radiolysis study on free radical scavenger edaravone (3-methyl-1-phenyl-2-pyrazolin- 5-one) 2: A comparative study on edaravone derivatives, K. Hata, M. Lin, Y. Katsumura, Y. Muroya, H. Fu, S. Yamashita, and H. Nakagawa, *J. Radiat. Res*. **52**, 15-23 (2011).
2) Fluorescent probe for steady-state radiolysis with heavy ions 1: LET effects and time dependence of OH yields, Y. Maeyama, S.Yamashita, G. Baldacchino, M.Taguchi, A. Kimura, Y. Katsumura, and T. Murakami, *Radiat. Phys. Chem*. **80**, 535-539 (2011).
3) Study on depth profile of heavy ion irradiation effects in poly(tetrafluoroethylene-co-ethylene), T. Gowa, T. Shiotsu, T. Urakawa, T. Oka, T. Murakami, A. Oshima, Y. Hama, and M. Washio, *Radiat. Phys. Chem*. **80**, 264-267 (2011).
4) Ortho-positronium reactions in water studied by positron annihilation age-momentum correlation, T. Hirade, T. Oka, and J. J. Lee, *Materials Sci. Forum* **666**, 103-108 (2011).
5) Electron paramagnetic resonance study of unpaired electron species in thin films of pyrimidine bases induced by nitrogen and oxygen K-shell photoabsorption, T. Oka, A. Yokoya, and K. Fujii, *Appl. Phys. Lett*. **98**, 103701-1-103701-3 (2011).
6) A novel technique using DNA denaturation to detect multiply induced single-strand breaks in a hydrated plasmid DNA molecule by X-ray and $^{4}He^{2+}$ ion irradiation, A. Yokoya, N. Shikazono, K. Fujii, M. Noguchi, and A. Urushibara, *Radiat. Protect. Dosim*. **143**, 219-225 (2011).
7) Model for analysis of the yield and the level of clustering of radiation-induced DNA strand breaks in hydrated plasmids, N. Shikazono, A. Yokoya, A. Urushibara, M. Noguchi, and K. Fujii, *Radiat. Protect. Dosim*. **143**, 181-185 (2011).
8) Development of function-graded proton exchange membrane for PEFC using heavy ion beam irradiation, F. Shiraki, T. Yoshikawa, A. Oshima, Y. Oshima, Y. Takasawa, N. Fukutake, T. Gowa Oyama, T. Urakawa, H. Fujita, T. Takahashi, T. Oka, H. Kudo, T. Murakami, Y. Hama, and M. Washio, *Nucl. Instr. Meth. Phys. Res. B* **269**, 1777-1781 (2011).
9) Induction of DNA DSB and its rejoining in clamped and non-clamped tumours after exposure to carbon ion beams in comparison to X rays, R. Hirayama, A. Uzawa, Y. Matsumoto, M. Noguchi, Y. Kase, N. Takase, A. Ito, S. Koike, K. Ando, R. Okayasu, and Y. Furusawa, *Radiat. Protect. Dosim*. **143**, 508-512 (2011).
10) Spin trapping reactions of a novel gauchetype radical trapper G-CYPMPO, T. Oka, S. Yamashita, S. Saiki, M. Midorikawa, Y. Muroya, M. Kamibayashi, M. Yamashita, K. Anzai, and Y. Katsumura, *Anal. Chem*. **83**, 9600-9604 (2011).
11) The mutagenic potential of 8-oxoG/single strand break-containing clusters depends on their relative positions, M. Noguchi, A. Urushibara, A. Yokoya, P. O'Neill, and N. Shikazono, *Mutation Res*. **732**, 34-42 (2012).
12) Yield of single- and double-strand breaks and nucleobase lesions in fully hydrated plasmid DNA films irradiated with high-LET charged particles, T. Ushigome, N. Shikazono, K. Fujii, R. Watanabe, M. Suzuki, C. Tsuruoka, H. Tauchi, and A. Yokoya, *Radiat. Res*. **177**, 614-627 (2012).

Books & Reviews
1) Radiation damage to DNA selectively induced by synchrotron X-rays, K. Fujii, *Radiation Effects Association* **2011.4**, 8-10 (2011) (*in Japanese*).

Invited Talks
1) Introduction to synchrotron radiation and radio-biological studies, A. Yokoya, *Surface Electro, Radiation, and Photo Chemistry International Master Course (SERP-Chem), EU Education & Training "ERASUMUS MUNDUS"*, Orsay, France (2011).
2) Spectroscopic studies of genome damage induced by ionizing radiation, A. Yokoya, *Summer school of the radiation section of the Japan Society of Applied Physics*, Sendai, Japan (2011).
3) Unpaired electron species in DNA and DNA-base thin films induced by K-shell photoabsorption, T. Oka, *Photon Factory Seminar: Prospect on Synchrotron Radiobiology focusing on Inhomogeneous Energy Deposition*, Tsukuba, Japan (2011).
4) Study of DNA damage using soft X-ray absorption technique, K. Fujii, *Photon Factory Seminar: Prospect on Synchrotron Radiobiology focusing on Inhomogeneous Energy Deposition*, Tsukuba, Japan (2011).
5) DNA base lesions induced by phosphorus K-ionization and its Auger decay, A. Yokoya, *Photon Factory Seminar: Prospect on Synchrotron Radiobiology focusing on Inhomogeneous Energy Deposition*, Tsukuba, Japan (2011).
6) Physicochemical processes of radiation damage to genomic DNA and its enzymatic repair, A. Yokoya, *67th Annual meeting of the Physical Society of Japan*, Nishinomiya, Japan (2012).

Research Group for Spin-Polarized Positron Beam

Papers
1) Development of pulsed positron beam with compact pulsing system, M. Maekawa and A. Kawasuso, *Nucl. Inst. Meth. Phys. Res*. B **270**, 23-27 (2011).
2) Positron annihilation study of 4H SiC by Ge+ implanted and subsequent thermal annealing, Y. Runsheng, M. Maekawa, A. Kawasuso, B. Y. Wang, and L. Wei, *Nucl. Inst. Meth. Phys. Res*. B **270**, 47-49 (2011).
3) Microstructure of nearly stoichiometric ZrC Coating layers for advanced high temperature gas cooled reactor fuel and positron annihilation spectroscopy of various ZrC coating layers, J. Aihara, M. Maekawa, S. Ueta, A. Kawasuso, and K. Sawa, *J. Am. Ceram. Soc*. **94**, 4516-4522 (2011).
4) Doppler broadening of annihilation radiation measurements on 3*d* and 4*f* ferromagnets using polarized positrons, A. Kawasuso, M. Maekawa, Y. Fukaya. A. Yabuuchi, and I. Mochizuki, *Phys. Rev*. B **85**, 024417-1-024417-6 (2012).
5) Increase in the beam intensity of the linac-based slow positron beam and its application at the Slow Positron Facility, KEK, K. Wada, T. Hyodo, A. Yagishita1, M. Ikeda, S. Ohsawa, T. Shidara, K. Michishio, T. Tachibana, Y. Nagashima, Y. Fukaya, M. Maekawa, and A. Kawasuso, *Eur. Phys. J*. D **66**, 37-40 (2012).

Researches conducted under collaborations between ASRC groups appear in each group's publication list. Excluding the overlap, the total number of papers is 179.

Appendix

◆ International Workshop

The 2nd ASRC International Workshop "Magnetic Materials and Nanostructures"
Date : January 10-13, 2012
Venue : Ricotti, Tokai, Japan
Organizers: T. Ziman (ILL, France), Y. J. Uemura (Columbia University, U.S.A)
URL: http://asrc.jaea.go.jp/soshiki/gr/mori-gr/workshop/mmn2011/index.html

The 3rd ASRC International Workshop "New Approach to the Exotic Phases of Actinide Compounds under Unconventional Experimental Conditions"
Date : January 31-Feburary 3, 2012
Venue : Institut Laue Langevin, Grenoble, France
Organizers: A. Hiess (ILL, France), G. H. Lander (ILL, France), S. Kambe (JAEA)
URL: http://www.ill.eu/news-events/past-events/2012/reimei/

The 4th ASRC International Workshop "Transformation of Radionuclides by Microorganisms, Clays, and Plants: Implication for Migration and Remediation"
Date : March 12-13, 2012
Venue : Ibaraki Quantum Beam Research Center, Tokai, Japan
Organizers: L. Macaskie (University of Birmingham, U.K), T. Ohnuki (JAEA)
URL: http://asrc.jaea.go.jp/soshiki/gr/mysite3/bio_ws/

The 5th ASRC International Workshop "Perspectives in Nuclear Fission"
Date : March 14-16, 2012
Venue : Ricotti, Tokai, Japan
Organizers: A. Andreyev (University of West Scotland, U.K), K. Nishio (JAEA)
URL: http://asrc.jaea.go.jp/fission_workshop/index.html

◆ ASRC Seminar

No.	Title	Speaker	Affiliation
436	Progress in the gamma spectroscopy of *p*-shell hypernuclei and the prospects for the *sd*-shell region	Toshio Motoba	Osaka Electro-Communication Universtiy
437	Functional analysis of nuclear non-coding RNAs in mammalian cells	Nobuyoshi Akimitsu	The University of Tokyo
438	Accident of the Fukushima Daiichi Nuclear Power Plant	Syunichi Tanaka	NPO Radiation Safety Fprum
439	Origin of spin-motive-forces	Stewart E. Barnes	University of Miami
440	Current status of Korea Isotope Accelerator	Yong Hee Chung	Hallym University
441	Iron-based n-type electron-induced ferromagnetic semiconductor	Pham Nam Hai	The Univertsity of Tokyo
442	7th JAEA Actinide Network workshop "Behavior of nuclear fission products in environment"	Toshihiko Ohnuki	JAEA
		Takumi Saito	The University of Tokyo
		Noriko Tomioka	National Institute for Environmental Studies
		Takeshi Matsunaga	JAEA
		Kazuya Tanaka	Hiroshima University
443	Hadron physics at LEPS and LEPS II	Masayuki Niiyama	Kyoto Universtiy
444	Shell structure and fission of exotic heavy nuclei	Satoshi Chiba Katsuhisa Nishio Hiroyuki Koura	JAEA
445	Extended Brueckner-Hartree-Fock theory in many body system-Importance of pion in nuclei -	Hiroshi Toki	Kyoto Universtiy
446	Thermoelectric materials and its applications	Yuzuru Miyazaki	Tohoku Universtiy
447	Description of heavy-ion fusion reactions near the Coulomb barriers based on a mean-field approximation	Kouhei Washiyama	Universite Libre de Bruxelles
448	Magnetic properties of lightly doped antiferromagnetic YBCO	Oleg P. Sushkov	The University of New South Wales
449	Study for nuclear medicine using the tandem accelerator of JAEA-Tokai -Aim at the new cancer medical treatment by α-emitting radioisotopes-	Ryouhei Amano	Kanazawa University
		Kohshin Washiyama	Kanazawa University
		Ichiro Nishinaka	JAEA
		Masahiko Watanabe	FUJIFILM RI Pharma CO., Ltd.
		Noriko Ishioka	JAEA
		Akihiko Yokoyama	Kanazawa University

450	Schottky barrier distribution in a single Fe/GaAs junction	Takafumi Hirohata	The University of York
451	Recent lattice QCD simulations on the *H*-dibaryon	Takashi Inoue	Nihon University
452	(1) The SISAK system and on-line liquid-liquid extraction (2) On-line LS alpha-detection system for continuous flow	Jon Petter Omtvedt	University of Oslo
453	^{237}Np Mössbauer studies on actinide superconductors and related materials	Eric Colineau	Institute for Transuranium Elements
454	Overview of the surrogate reactions program at LLNL	Jason Burke	Lawrence Livermore National Laboratory
455	Experimental studies of hot and dense QCD medium at LHC-ALICE	Taku Gunji	The University of Tokyo
456	Theory of charmed deuterons	Makoto Oka	Tokyo Institute of Technology
457	A current review for study of hidden ordering in URu_2Si_2	Hiroshi Amitsuka	Hokkaido University
	Electronic state of hidden ordered phase in URu_2Si_2	Michito Suzuki	JAEA
	Non-Magnetic Kondo effect emerging from vibrating magnetic ion	Takashi Hotta	Tokyo Metropolitan University
458	Temperature can enhance coherent oscillations at a Landau-Zener transition	Timothy Ziman	Institut Laue-Langevin
459	New radioactive ion beams at CERN-ISOLDE : Target and ion source developments	Thierry Stora	CERN
460	Spin excitations in cuprates and iridates probed by resonant x-ray scattering	Giniyatulla Khaliullin	Max-Planck Institut
461	Biological assessment of radiation damage of ATP induced by soft X-rays	Kentaro Fujii	JAEA
		Shin-ichiro Fujii	Agency of Industrial Science and Technology
		Dai Kato	Agency of Industrial Science and Technology
		Mitsutoshi Tsukimoto	Tokyo University of Science
		Nobuyoshi Akimitsu	The University of Tokyo
462	Electric-field control of the magnetic exchange interaction in quantum dots and molecules	Jan Martinek	Polish Academy of Sciences
463	Spin excitation and phonon effect for spin-Peierls model	Takanori Sugimoto	Kyoto University
464	Laser ionization spectroscopy of exotic nuclei; Recent results from the ISOLDE-CERN and LISOL facilities	Piet van Duppen	University of Leuven
465	Search for neutron-rich Lambda hypernuclei at J-PARC	Atsushi Sakaguchi	Osaka University
466	Quantum critical behavior and field-induced superconducting phase in $CeCoIn_5$ investigated by the magnetocaloric effects	Yoshifumi Tokiwa	University of Goettingen
467	Theoretical research on the structural and transport characteristics of several functional nanowires	Zhuo Xu	Chinese Academy of Science
468	Drawing a nuclear phase diagram by high-energy heavy-ion reactions	Takao Sakaguchi	Brookhaven National Laboratory

◆ Research themes accepted for Reimei Research Program 2011

Research Theme	Project Director (Applicant)	Organization
New approach to the exotic phases of actinides compounds under unconventional experimental conditions	Arno Hiess	Institut Laue Langevin
New fission mechanism peculiar to proton-rich nuclei	Andrei Andreyev	University of the West of Scotland
Exploration of new biological specific function by heavy elements stimulus	Lynne E. Macaskie	University of Birmingham
Synthesis, magnetic and transport studies of Li(Zn,Mn)As and other doped I-II-V magnets	Yasutomo J. Uemura	Columbia University
Theoretical studies in spintronics and multifunctional materials	Timothy Ziman	Institut Laue Langevin

◆ Research Collaborations and Cooperations

The number of Research collaborations	
Research collaborations	37
Research cooperations	3

The number of organizations based on joint research arrangements	
Universities	21
Public Institutes	7
Others	7
Foreign Organizations	12

Japan Atomic Energy Agency

Advanced Science Research Center

2-4 Shirakata Shirane, Tokai-mura, Naka-gun, Ibaraki Pref. 319-1195
http://asrc.jaea.go.jp/asr_eng/